Accepted Manuscript

Novel dual inhibitors targeting CDK4 and VEGFR2 synergistically suppressed cancer progression and angiogenesis

Zhi Huang, Borui Zhao, Zhongxiang Qin, Yongtao Li, Tianqi Wang, Wei Zhou, Jianyu Zheng, Shengyong Yang, Yi Shi, Yan Fan, Rong Xiang

PII: S0223-5234(19)30665-8

DOI: https://doi.org/10.1016/j.ejmech.2019.07.044

Reference: EJMECH 11541

To appear in: *European Journal of Medicinal Chemistry*

Received Date: 15 April 2019

Revised Date: 13 July 2019

Accepted Date: 14 July 2019

Please cite this article as: Z. Huang, B. Zhao, Z. Qin, Y. Li, T. Wang, W. Zhou, J. Zheng, S. Yang, Y. Shi, Y. Fan, R. Xiang, Novel dual inhibitors targeting CDK4 and VEGFR2 synergistically suppressed cancer progression and angiogenesis, *European Journal of Medicinal Chemistry* (2019), doi: https://doi.org/10.1016/j.ejmech.2019.07.044.

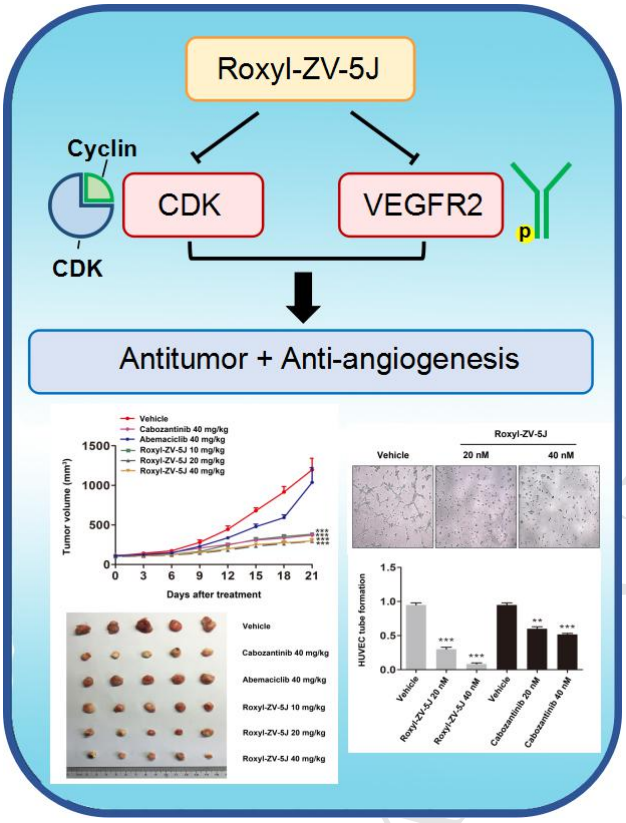

A novel dual inhibitor, **Roxyl-ZV-5J** with potent and balanced activities against both CDK4 and VEGFR2 at the nanomolar level, exhibited improved antitumor and anti-angiogenesis activities over positive drugs *in vitro* and *in vivo*.

Novel dual inhibitors targeting CDK4 and VEGFR2 synergistically suppressed cancer progression and angiogenesis

Zhi Huang [a, b #], Borui Zhao [a,f #], Zhongxiang Qin [a], Yongtao Li [a], Tianqi Wang [a], Wei Zhou [a], Jianyu Zheng [d], Shengyong Yang [e], Yi Shi [a, b]*, Yan Fan [a, b]* and Rong Xiang [a, b, c] *

[a] Department of Medicinal Chemistry, School of Medicine, Nankai University, 94 Weijin Road, Tianjin 300071, China

[b] 2011 Project Collaborative Innovation Center for Biotherapy of Ministry of Education, 94 Weijin Road, Tianjin 300071, China

[c] State Key Laboratory of Medicinal Chemical Biology, 94 Weijin Road, Tianjin 300071, China

[d] State Key Laboratory and Institute of Elemento-Organic Chemistry, Collaborative Innovation Center of Chemical Science and Engineering, Nankai University, Tianjin 300071, China

[e] Medical Oncology, Cancer Center, State Key Laboratory of Biotherapy, West China Hospital, Sichuan University, Chengdu, China

*** Corresponding authors:*** Yi Shi, E-mail: yishi@nankai.edu.cn * Yan Fan, E-mail: yanfan@nankai.edu.cn; Rong Xiang*: E-mail: rxiang@nankai.edu.cn.

Author Contributions: [#]Zhi Huang and Borui Zhao are contributed equally to this work.

Abstract

Based on the significantly synergistic effects of CDK4 and VEGFR2 inhibitors on growth of cancer cells, a series of novel multi-kinase inhibitors targeting CDK4 and VEGFR2 were designed, synthesized and evaluated, among which **Roxyl-ZV-5J** exhibited potent and balanced activities against both CDK4 and VEGFR2 with half-maximal inhibitory concentration at the nanomolar level. It effectively induced breast and cervical cancer cell cycle arrest and cell apoptosis. **Roxyl-ZV-5J** also inhibited the proliferation, tube formation and VEGFR2 downstream signaling pathways of HUVECs. Oral administration of **Roxyl-ZV-5J** led to significant tumor regression and anti-angiogenesis without obvious toxicity in SiHa xenograft mouse model. In addition, this compound showed good pharmacokinetics. This study confirmed a new tool for dual CDK-VEGFR2 pathways inhibition achieved with a single molecule, which provided valuable leads for further structural optimization and anti-angiogenesis and anti-tumor mechanism study.

Keywords: CDK4, VEGFR2, Inhibitor, Cancer

1. Introduction

Cancer is a multigenetic disease involving multiple cross-talks between signaling networks and often required multiple therapeutic interventions[1]. Kinase inhibitors are widely employed in clinical oncology as molecularly targeted therapeutics and lead for drug design. Simultaneous inhibition of multiple mechanisms can yield superior efficacy, such as synergy effects, as exemplified by multi-kinase inhibitors [2]. The utility of these inhibitors simultaneous targeting multiple pathways is critical for tumor proliferation, angiogenesis and apoptotic regulation[3].

More recently the promising target to control tumor cellular proliferation is inhibition of cell cycle progression by targeting cyclin-dependent kinases (CDKs)[4, 5]. Different CDKs forming complexes with cyclins control specific checkpoint of the cell cycle, which have two major functional groups based on their roles. The subtypes 1-4 and 6 of CDKs mainly mediate cell cycle and subtypes 5, 7-9 of CDKs regulate transcription control [6]. Aberrations in CDKs-cyclin pathway have been observed in various tumors, including those of the breast, colon, liver and brain. The simultaneous and pharmacological inhibition of these kinases have been proved to provide an effective approach for cancer compared with the inhibition of a single CDK alone [7, 8].

Multiple generations of drugs targeting CDK have been designed and synthesized through binding in the ATP-binding cleft of CDK enzymes. More recently, third-generation CDK-directed drugs targeting CDK4/6, palbociclib, ribociclib and

abemaciclib have received significant attention [9-13]. But in clinical trials, these compounds needed to combine with letrozole or tamoxifen for the treatment of $ER^+/HER2^-$ metastatic breast cancer, which indicated a lack of sensitivity to CDK4/6 monotherapy[14, 15]. Therefore, we reasoned that development of single drug with multiple biological targets based on CDK4/6 to improve efficacy in cancer treatment.

Angiogenesis is required for the growth, survival, and metastasis of most solid tumors, including breast cancer [16]. Of all angiogenic molecules, vascular endothelial growth factor (VEGF) is the primary modulator of angiogenesis and metastasis in human carcinogenesis. Therapies that block VEGF signaling has been demonstrated to retard angiogenesis and inhibit tumor growth [17, 18]. VEGF executes its effects by binding to and activating its receptors (VEGFRs). In endothelial cells, VEGFR2 is the major regulator of VEGF-stimulated cell survival and vascular permeability during angiogenesis [19]. It has been reported that VEGFR2 inhibitors possess synergistic anti-tumor effects in rational combinations with anti-cancer drugs [20, 21]. Recent research indicated that concurrent of cell cycle arrest and angiogenesis inhibition showed more effective due to synergy effects [8, 22-26].

Cabozantinib is a highly potent small molecule inhibitor against VEGFR2 [27, 28]. In a recent study, we developed a novel hybrid inhibitor based on LEE011 and cabozantinib structure, which indeed showed a much higher anti-tumor activity than positive drugs both *in vitro* and *in vivo*. Nevertheless, the compound show low inhibition effect targeting VEGFR2 [29]. In our continued effort to discover novel

dual-action inhibitors targeting both CDK4 and VEGFR2, a series of compounds were designed and synthesized based on the remarkably synergistic effects of CDK4 inhibitor and VEGFR2 inhibitor on growth of cancer cell lines (**Figure S1**). To the most active compound in enzymatic and cellular assays, an in depth anti-tumor activities both *in vitro* and *in vivo* are evaluated. (**Figure 1**)

2. Results and discussions

2.1 Chemistry

All compounds prepared by routes were outlined in **Schemes 1−3**. **Scheme 1** outlines the routes of compounds **5A-K, 6D, 6F, 6H, 6J, 6K.** Briefly, compounds **5A-K, 6D, 6F, 6H, 6J** and **6K** were synthesized from cyclopropane-1,1-dicarboxylic acid condensation with aniline or substituted aniline [29, 30]. The condensation of *p*-phenylenediamine or 4-(aminomethyl)aniline dihydrochloride with carboxylic acids **2A-K** afforded **3A-K, 4D, 4F, 4H, 4J** and **4K** under condensing agent 1-Ethyl-3-(3-dimethyllaminopropyl)carbodiimide hydrochloride (EDCI) in the presence of 1-hydroxybenzotriazole (HOBt), N,N-diisopropylethylamine (DIEA) [29, 31]. A palladium catalyzed cross-coupling reaction of compounds **3A-K, 4D, 4F, 4H, 4J** and **4K** with compound 6-(2-chloro-5-fluoropyrimidin-4-yl)-4-fluoro-1-isopropyl-2-methyl-1H-benzo[d]imidazole(**7**) provided compounds **5A-K** and **6D, 6F, 6H, 6J, 6K**, respectively [29, 32].

We synthesized the key intermediate **13** and the general synthetic routes are illustrated in **Scheme 2**. Firstly, commercial compound 4-bromo-2-fluoro-1–

nitrobenzene (**8**) reacted with isopropylamine to provide compound **9**. Secondly, compound **9** was reduced to amino group. Compound **11** was obtained by closing the ring in the presence of conc.HCl and aq $NaNO_2$ [33]. Finally, compound **11** was converted to the corresponding heteroarylboronate ester (**12**) which underwent palladium catalyzed Suzuki reaction with 2, 4-dichloro-5-fluoropyrimidine to yield **13**. **Scheme 3** outlines the routes used to synthesize compounds **14A-K.** A palladium catalyzed cross-coupling reaction of compounds **3A-K** with compound 6-(2-chloro-5-fluoropyrimidin-4-yl)-1-isopropyl-1H-benzo[d][1,2,3]triazole (**13**) provided compounds **14A-K**, respectively.[29, 32]

2.2 Enzyme Inhibitory Activity and SAR

Based on the synergistic experimental results with mean CI < 1 across relevant concentrations of CDK4/6 inhibitors ribociclib or abemaciclib, with VEGFR2 inhibitor cabozantinib *in vitro* (**Figure S1**), we initiated our hybrid strategy to merge two different pharmacophores to link two inhibitors together to obtain compounds **4d**, **5B** . Enzymatic-based assays were preliminarily to evaluate the bioactivity of the synthesized compounds in the SAR studies. As shown in **Table 1**, substitutions at the part 1 position substantially impacted the activity. Compared with pharmacophore Y, pharmacophore X all increased both CDK4 and VEGFR2 inhibitory activities, revealing that pharmacophore X of abemaciclib are optimal substituent for our dual inhibitor design. Subsequently, we fixed part 1 as X group and varied the part 3 group substituent. Compared with **5A**, when R_2 position is CF_3, compounds **5G**, **5H** decreased CDK4 inhibitory activities (31% and 74%, respectively), revealing that the

electron-withdrawing group may decrease the inhibition activity of CDK4. Other compounds with CF_3 substituent at R_2 position (**5K** and **4l**) were similar activities against CDK4. On the contrary, compounds with the electron-donating group CH_3 substituent at R_2 position (**5I** and **5J**) are more active, which indicated that the electron-donating group should be beneficial for enhancing the inhibition activity of CDK4. We then explored the influence of different substituents on part 2. According to the structural characteristic of abemaciclib, we introduced a CH_2 group to synthesize **6D**, **6F** and **6J**. Compared with compounds **5D**, **5F** and **5J**, compounds **6D**, **6F** and **6J** showed parallel potency against CDK4. As expected, compounds **6H** and **6K** with electron-withdrawing groups at R_2 position exhibited low binding affinity. Furthermore, we reconstructed the X group to obtain the Z group and synthesized 11 derivatives **14A-K**. These compounds were all inactive against either CDK4 or VEGFR2 at the test concentration (1 μM). It implied that X group is the most suitable substituent among these three groups of Part 1. It was worth noting that compounds **14G**, **14H** and **14K** containing electron-withdrawing group CF_3 exhibited obviously lower inhibition activity against both CDK4 and VEGFR2, compared with compounds **14I** and **14J** containing electron-donating group CH_3. These results were consistent with the above conclusions: the electron-donating group is favorable for the inhibition activity of CDK4.

Compounds with Y and Z group at part 1 were inactive against VEGFR2 in **Table 1**, Therefore, X group is beneficial for inhibition of VEGFR2 activity. From **Table 1**, we can see that the derivatives with CF_3 at part 3 position have in-activities in enzymatic

level. These data clearly show substitution of R_2 by CH_3 is the most optimal. We identified dual-acting compounds **5A**, **5B, 5F, 5I**, **5J, 6F** and **6J** exhibiting better kinase inhibitory among the derivatives.

The reason was further described that **Figure 2A** shows a docking model between **5J** and CDK4. It can be seen from the diagram that **5J** forms a hydrogen bond between NH and an oxygen atom in 12-position isoleucine. The substituents of benzene ring were electron-withdrawing groups, which reduced the density of electron cloud of nitrogen atom in NH. It made hydrogen atom closer to nitrogen atom. This increased the distance between NH and an oxygen atom of 12-position isoleucine, thus lowering the hydrogen bonding and ultimately decreasing the activity. However, the substituents on benzene ring were electron donating groups, which increased the electron cloud density of nitrogen atoms in NH. It made hydrogen atom in NH closer to an oxygen atom of 12-position isoleucine, thus enhancing the hydrogen bonding and eventually increasing inhibition activity of CDK4.

2.3 Cellular Assay.

As the aim of this study was to discover dual-action inhibitors targeting both CDK4 and VEGFR2 for cancer treatment, we screened compounds exhibiting better kinase inhibitory to do the preliminary cell inhibition assays. Compounds **5A**, **5B, 5F, 5I**, **5J, 6F** and **6J** were chosen to test their cellular cytotoxic activity (**Figure S2 and S3**). We found that compound **5J** had significant cancer cell inhibitory activity. We further evaluated the effect of compound **5J** on proliferation in cervical cancer cell lines

(SiHa and HeLa), breast cancer cell lines (MDA-MB-231 and T-47D) (**Table 2**). Compound **5J** potently inhibited the growth of cervical cancer cells and breast cancer cells. These results demonstrated that **Roxyl-ZV-5J** performed better inhibitory ability compared to cabozantinib or abemaciclib. The best tumor cell potency of these analogues was obtained for compound **5J**, which displayed inhibition of CDK4 and VEGFR2 with IC_{50} values of 46 nM and 46 nM, respectively (Figure **S4)**. Therefore, as attributed of a truly merged bispecific pharmacophore and the results of anti-tumor activity in cells, **Roxyl-ZV-5J** was chosen for further studies both *in vitro* and *in vivo* subsequently.

2.4 Lipophilicity.

Log P and Log D describe a compound's lipophilicity, and often correlate with a number of key biopharmaceutical parameters in drug discovery. We detected the concentration of **Roxyl-ZV-5J** in the aqueous and organic phases and calculated Log P (Log $D_{7.4}$) value. The values were measured using the traditional shake flask method. The Log P value for **Roxyl-ZV-5J** is 2.53 and Log $D_{7.4}$ value is 2.51. Our results indicated that compound **Roxyl-ZV-5J** has a good lipophilicity.

2.5 Kinase Selectivity Profiling.

To characterize the kinase inhibitory activities and selectivity, kinase inhibition profiling assays with a fixed concentration of 1 μM of compound **Roxyl-ZV-5J** were carried out against a series of 270 kinases through the Eurofins kinase profiling. The

results are shown in **Table S1**. Compound **Roxyl-ZV-5J** did not show obvious activity against other kinases, indicated acceptable kinase selectivity.

2.6 Molecular Modeling of Compound Roxyl-ZV-5J

Molecular docking studies were carried out to investigate the binding modes of compound **Roxyl-ZV-5J** in CDK4 and VEGFR2, respectively. **Figure 2** illustrated the predicted binding modes and the detailed protein-inhibitor interactions of compound **Roxyl-ZV-5J** with CDK4 and VEGFR2, respectively. For comparison, the binding mode of **Roxyl-ZV-5J** was superimposed on that of abemaciclib and cabozantinib. Our results showed that compound **Roxyl-ZV-5J** is a potent inhibitor of CDK4 with an IC_{50} of 46 nM. As shown in **Figure 2A** and **2B**, **Roxyl-ZV-5J** could tightly bind to the ATP-binding site of CDK4 in a binding mode. Hydrogen bonds appear to be formed between the aminopyrimidine and the backbone residue of VAL96 and ASP97. These hydrogen bonds are critical for binding to CDK4. The crystal structure of VEGFR2 was taken from the RCSB Protein Data Bank (PDB code: 2OH4). As shown in **Figure 2C** and **2D**, **Roxyl-ZV-5J** could tightly bind to the ATP-binding site of VEGFR2 in a binding mode. In this binding model, hydrogen bonds between the hinge-region CYS 917 and the fluorine atom of the pyrimidine ring were observed. Moreover, carbonyl oxygen could form significant hydrogen bond with the backbone NH of ASP 1044. Other hydrogen bond interaction was formed between the residue GLU883 and the NH of **Roxyl-ZV-5J**, which indicated **Roxyl-ZV-5J** would be a good inhibitor for VEGFR2.

2.7 Roxyl-ZV-5J inhibited the tube formation and VEGFR2 downstream signaling pathways of HUVECs *in vitro*.

The compound **Roxyl-ZV-5J** was next evaluated in a dose response study to against HUVEC, with cabozantinib, abemaciclib or Vehicle as control groups. Values of IC_{50} measured after 72 h were presented in **Table 2**. The results showed a significantly higher drug activity of **Roxyl-ZV-5J** with IC_{50} around 40 nM. However, cabozantinib or abemaciclib presented IC_{50} almost >400 nM. Hence, we selected 20 nM and 40 nM as research concentrations of HUVECs, then cell viability was examined after treated with **Roxyl-ZV-5J** 20 nM, 40 nM, cabozantinib 40 nM, abemaciclib 40 nM or Vehicle at 0, 12, 24, 36, 48, 60 and 72 h. The results indicated that **Roxyl-ZV-5J** effectively inhibited cell viability in dose- and time-dependent manner compared to other groups (**Figure 3A**). Although angiogenesis involved several types of cells, tube formation in endothelial cells was a significant step. After treated with different concentrations of **Roxyl-ZV-5J**, cabozantinib or vehicle for 6 h, HUVECs were observed under a light microscope. It was confirmed that **Roxyl-ZV-5J** could effectively attenuate the ability of tube formation of HUVECs compared to cabozantinib or Vehicle group (**Figure 3B**). To determine whether **Roxyl-ZV-5J** inhibited VEGFR2 and its downstream signaling pathways, we screened essential kinases involved in VEGFR2 signaling. Western Blot assay showed that **Roxyl-ZV-5J** treatment suppressed VEGFR-mediated phosphorylation of VEGFR2, STAT3, Akt and Src, while phosphorylation of Erk1/2 barely altered (**Figure 3C**).

2.8 Roxyl-ZV-5J restrained angiogenesis *in vivo*

We conducted Matrigel plug assay in a mouse model of angiogenesis. As shown in **Figure 4**, the subcutaneous new blood vessels of Balb/c mice were significantly inhibited in **Roxyl-ZV-5J** groups compared to cabozantinib or vehicle group. The results revealed that **Roxyl-ZV-5J** blocked new blood vessel formation *in vivo*.

2.9 Roxyl-ZV-5J suppressed the proliferation of cancer cells.

Colony formation assay confirmed that **Roxyl-ZV-5J** had a robust growth inhibition on MDA-MB-231, T-47D, SiHa and HeLa cells when comparing to other treatments (**Figure 5A**). Moreover, EdU assay demonstrated that the positive ratio of proliferating cells was decreased after treated with **Roxyl-ZV-5J** compared to other groups (**Figure 5B**).

2.10 Roxyl-ZV-5J modulated cell cycle arrest *in vitro*.

We wondered whether the inhibitory of cell proliferation partly result cell cycle inhibition. We next investigated the effect of **Roxyl-ZV-5J** treatment on cell cycle kinetics. As shown in **Figure 6**, the FACS analysis revealed that abemaciclib treatment resulted in accumulation of cells in G_0/G_1 phase, while treatment of cabozantinib presented a mildly G_2 arrest. **Roxyl-ZV-5J** significantly induces G_2 arrest, accompanied by decreases in S phase **(Figure 6A**). As reported, the G2 phase inhibition was indicative of cells undergoing apoptosis, which attributed to the role for inhibition of VEGFR2 [34, 35]. Accumulation of cells in G2/M phase is a significant remark of the apoptotic role of compound **Roxyl-ZV-5J** in cells. The results

confirmed that compound **Roxyl-ZV-5J** had anti-proliferative properties.

2.11 Roxyl-ZV-5J induced cell apoptosis *in vitro*.

Subsequently, the effect of **Roxyl-ZV-5J** on cell apoptosis was conducted using Annexin V and PI double staining. Treatment with **Roxyl-ZV-5J** markedly increased Annexin V positive early-stage and late-stage apoptotic cells, compared with control groups (**Figure 6B**). Western Blots assay indicated that **Roxyl-ZV-5J** decreased the expression level of p-Rb in dose-dependence. Meanwhile, **Roxyl-ZV-5J** depressed the proliferation associated protein Ki67 expression (**Figure 6C**). **Roxyl-ZV-5J** also suppressed the expression level of apoptosis associated proteins Bcl-2 compared to other groups. These above results showed that the inhibition of cancer cell growth induced by **Roxyl-ZV-5J** was associated with cell cycle and apoptosis, confirming the existence of multi-intracellular targets.

2. 12. Roxyl-ZV-5J inhibited tumor growth and angiogenesis *in vivo*.

To better assess whether **Roxyl-ZV-5J** could efficiently inhibit tumor growth and angiogenesis *in vivo*, we constructed xenograft models using Nod/SCID female mice bearing SiHa cells. Mice were sacrificed at day 21, tumor growth curve demonstrated that **Roxyl-ZV-5J** (10 mg/kg, 20 mg/kg, 40 mg/kg) treatments were effective compared to cabozantinib and abemaciclib 40 mg/kg or vehicle group, especially in **Roxyl-ZV-5J** 20 mg/kg and 40 mg/kg group (**Figure 7A**). The average body weight of mice was monitored every 3 days after gavage. There were hardly changed in cabozantinib or abemaciclib group, while in **Roxyl-ZV-5J** 20 mg/kg and 40 mg/kg

group, body weight of mice slightly decreased (**Figure 7B**). An obvious decrease in tumor weight and volume was also observed at the end-point of the study (**Figure 7C** and **7D**).As Ki67 and CD31 presented the markers of proliferation and angiogenesis respectively, IHC staining showed that the expression level of Ki67 and CD31 was obviously suppressed in **Roxyl-ZV-5J** groups in dose-dependence (**Figure 7E**). In addition, acute general toxicity analysis indicated that **Roxyl-ZV-5J** did not induce any toxic effects on mice compared to control group (**Figure S5**). These results demonstrated that **Roxyl-ZV-5J** effectively inhibited tumor growth and angiogenesis of xenograft tumor mice without obvious toxicity.

2.13. Pharmacokinetic Characteristics of Roxyl-ZV-5J in Rats.

Pharmacokinetic evaluation in rats following intravenous and oral administration of **Roxyl-ZV-5J** was further evaluated (**Table 3**). Compound **Roxyl-ZV-5J** showed good oral bioavailability of 60%. The oral maximum plasma concentration (Cmax) was 1.47 mg/L. Besides, compound **Roxyl-ZV-5J** showed oral apparent distribution volume (Vss) of 5.901 L/kg and a clearance of 1.589 L/h/kg. All of these results indicated that **Roxyl-ZV-5J** presented favorable pharmacokinetic properties, which may be a promising lead compound for the treatment of tumor diseases.

3. Conclusion

As reported, broad-spectrum inhibitors have exemplified superior efficacy compared with traditional agents, with increasing use in clinical oncology as molecular targeted therapeutics. The efficacy of these drugs is often simultaneously

targeting multiple pathways that are critical for cancer growth, including those that promote proliferation, angiogenesis, and apoptotic regulation.

In our present work, based on the favorable synergistic effects between CDK4 and VEGFR2 inhibitors, a series of cyclopropane-1, 1-dicarboxamide derivatives as CDK4 and VEGFR2 dual inhibitors were designed, synthesized, and evaluated. The representative compound **Roxyl-ZV-5J** simultaneously inhibited the oncogenic kinases CDK4 and VEGFR2, leading to much potent anti-proliferative and anti-angiogenesis capacities. **Roxyl-ZV-5J** displayed prominent cytotoxic activity in various cancer cell lines with IC_{50} values in the 16−70 nM range, several times lower than that for the reference drugs. **Roxyl-ZV-5J** induced G2/M phase arrest and inhibited cancer cell proliferation, as shown in the EdU-incorporation assay. To understand the mechanism of action of **Roxyl-ZV-5J**, we identified important mediators related to the pathways, such as the cell cycle, apoptosis and angiogenesis. **Roxyl-ZV-5J** demonstrated effective inhibition of CDK and VEGFR2 signaling pathways in the relevant *in vitro* and *in vivo* models examined. It was much more potent than abemaciclib in inhibiting phosphorylation of Rb protein and than cabozantinib in inhibiting angiogenesis. In addition, **Roxyl-ZV-5J** significantly inhibited the relative levels of Ki67. We demonstrated that **Roxyl-ZV-5J** induced apoptosis in solid tumour cells, which reduced expression of the antiapoptotic protein BCL-2.*In vivo*, oral administration of **Roxyl-ZV-5J** with 20 mg/kg or 40 mg/kg every day showed significant anti-tumor potency and no obvious toxicity.

In summary, **Roxyl-ZV-5J** possessed acceptable kinase selectivity and good

pharmacokinetics. As a mutitarget inhibitor, **Roxyl-ZV-5J** is noteworthy because the combined inhibition of transcriptional CDK with cell-cycle regulation and VEGFR2 with angiogenesis regulation has been shown to be advantageous for effective apoptotic induction in tumor cells. The merit of our research is the development of a series of CDK4 and VEGFR2 dual inhibitors with excellent anti-tumor and anti-angiogenesis activity, which validated the biology-oriented multitarget drug design strategy.

4. Experimental

4.1 Chemistry

^{1}H NMR (400 MHz), ^{13}C NMR (101 MHz) and ^{19}F NMR(376 MHz) spectra were taken on a Bruker AV-400 MHz spectrometer and chemical shifts were reported in ppm downfield from internal Me_4Si. Melting points (mp) were taken in open capillaries on a Mettler MP 50 melting-point system. High-resolution mass spectra (HRMS) were recorded on a VG ZAB-HS mass spectrometer under electron spray ionization (ESI). All of the solvents were purified and distilled according to the standard procedure. The commercially obtained materials were used directly without further purification unless otherwise noted.

The purity of tested compound was assessed to be ≥ 95% by HPLC analysis on a Shimadzu Prominence-i LC-2030C 3D system (column, InertSustain C_{18}, 4.6 mm × 250 mm, 5 μm; mobile phase, gradient elution of methanol/H_2O; low rate, 1.0 mL/min; UV wavelength, 190−800 nm; temperature, 40 °C; injection volume, 10 μL).

4.1.1. General Procedure for the Preparation of **2A-P**. To a stirred solution of cyclopropane-1,1-dicarboxylic acid (**1**) (13.01 g, 100 mmol) in isopropyl acetate (150 mL) at 0□, thionyl chloride (12.5 g, 105 mmol) was added dropwise. After addition, the resulting mixture was stirred at room temperature and stirred for 6 hours. The resulting mixture was then treated with a solution of aniline or substituted aniline (110 mmol) and triethylamine (110 mmol) in isopropyl acetate (40 mL) over 1 hour. After stirred for 2 hours, the resulting mixture was added ethyl acetate (500 mL). The solvent was washed by 1 N HCl solution and brine. The organic phase was dried over MgSO4, evaporated and the residue treated with heptane (200 mL). The product slurry was stirred for 0.5 h, filtered and dried under vacuum to obtain product.

4.1.1. General Procedure for the Preparation of **2A-K**. To a stirred solution of cyclopropane-1,1-dicarboxylic acid (**1**) (13.01 g, 100 mmol) in isopropyl acetate (150 mL) at 0□, thionyl chloride (12.5 g, 105 mmol) was added dropwise. After addition, the resulting mixture was stirred at room temperature and stirred for 6 hours. The resulting mixture was then treated with a solution of aniline or substituted aniline (110 mmol) and triethylamine (110 mmol) in isopropyl acetate (40 mL) over 1 hour. After stirred for 2 hours, the resulting mixture was added ethyl acetate (500 mL). The solvent was washed by 1 N HCl solution and brine. The organic phase was dried over MgSO4, evaporated and the residue treated with heptane (200 mL). The product slurry was stirred for 0.5 h, filtered and dried under vacuum to obtain product.

4.1.1.1. 1-((3-fluorophenyl)carbamoyl)cyclopropane-1-carboxylic acid (**2A**). White solid (76%), ^{1}H NMR (400 MHz, DMSO-d_6) δ 13.12 (s, 1H), 10.73 (s, 1H), 7.61 (dt, *J*

= 11.3, 2.0 Hz, 1H), 7.41 – 7.27 (m, 2H), 6.88 (ddt, *J* = 9.1, 6.7, 2.7 Hz, 1H), 1.41 (s, 4H).

4.1.1.2.1-((4-fluorophenyl)carbamoyl)cyclopropane-1-carboxylic acid (**2B**). White solid (67%), ^{1}H NMR (400 MHz, DMSO-d_6) δ 13.11 (s, 1H), 10.81 – 10.50 (m, 1H), 7.63 (dd, *J* = 8.9, 5.0 Hz, 2H), 7.13 (tt, *J* = 8.9, 3.0 Hz, 2H), 1.54 – 1.30 (m, 4H).

4.1.1.3.1-((3-chlorophenyl)carbamoyl)cyclopropane-1-carboxylic acid (**2C**). White solid (81%), ^{1}H NMR (400 MHz, DMSO-d_6) δ 13.12 (s, 1H), 10.70 (s, 1H), 7.83 (t, *J* = 1.9 Hz, 1H), 7.46 (d, *J* = 8.2 Hz, 1H), 7.32 (td, *J* = 8.1, 1.5 Hz, 1H), 7.10 (dd, *J* = 7.9, 2.1 Hz, 1H), 1.42 (s, 4H); ^{13}C NMR (101 MHz, DMSO) δ 173.52, 167.03, 140.20, 133.04, 130.33, 123.03, 118.79, 117.69, 28.87, 16.98.

4.1.1.4.1-((4-chlorophenyl)carbamoyl)cyclopropane-1-carboxylic acid (**2D**). White solid (55%), ^{1}H NMR (400 MHz, DMSO-d_6) δ 13.10 (s, 1H), 10.65 (s, 1H), 7.71 – 7.54 (m, 2H), 7.49 – 7.23 (m, 2H), 1.41 (s, 4H); ^{13}C NMR (101 MHz, DMSO) δ 173.60, 166.80, 137.75, 128.56, 126.87, 120.85, 28.80, 16.95.

4.1.1.5.1-((3-bromophenyl)carbamoyl)cyclopropane-1-carboxylic acid (**2E**). White solid (76%), ^{1}H NMR (400 MHz, DMSO-d_6) δ 13.12 (s, 1H), 10.69 (s, 1H), 7.97 (t, *J* = 2.0 Hz, 1H), 7.50 (dt, *J* = 7.5, 1.9 Hz, 1H), 7.39 – 7.15 (m, 2H), 1.42 (s, 4H); ^{13}C NMR (101 MHz, DMSO) δ 174.03, 167.51, 140.83, 131.13, 126.43, 122.14, 122.01, 118.57, 29.38, 17.50.

4.1.1.6.1-((4-bromophenyl)carbamoyl)cyclopropane-1-carboxylic acid (**2F**). White solid (84%), ^{1}H NMR (400 MHz, DMSO-d_6) δ 13.13 (s, 1H), 10.70 (s, 1H), 7.64 –

7.55 (m, 2H), 7.51 – 7.41 (m, 2H), 1.43 (s, 4H); ^{13}C NMR (101 MHz, DMSO) δ 174.22, 167.32, 138.61, 131.95, 121.73, 115.43, 29.15, 17.70.

4.1.1.7.1-((3-(trifluoromethyl)phenyl)carbamoyl)cyclopropane-1-carboxylic acid (**2G**). White solid (81%), ^{1}H NMR (400 MHz, DMSO-d_6) δ 13.13 (s, 1H), 10.83 (s, 1H), 8.13 (t, *J* = 1.9 Hz, 1H), 7.95 – 7.72 (m, 1H), 7.53 (t, *J* = 8.0 Hz, 1H), 7.46 – 7.30 (m, 1H), 1.43 (s, 4H); ^{13}C NMR (101 MHz, DMSO) δ 173.92, 167.75, 140.04, 130.39, 130.34, 130.08, 129.77, 129.45, 128.60, 125.89, 123.33, 123.18, 120.13, 120.09, 115.89, 115.85, 29.49, 17.34.

4.1.1.8.1-((4-(trifluoromethyl)phenyl)carbamoyl)cyclopropane-1-carboxylic acid (**2H**). Yellow solid (82%), ^{1}H NMR (400 MHz, DMSO-d_6) δ 12.95 (s, 1H), 10.91 (s, 1H), 7.82 (d, *J* = 8.5 Hz, 2H), 7.65 (d, *J* = 8.5 Hz, 2H), 1.44 (s, 4H); ^{13}C NMR (101 MHz, DMSO) δ 174.04, 167.78, 142.80, 126.48, 126.45, 126.41, 126.13, 124.03, 123.71, 123.43, 119.65, 29.44, 17.55.

4.1.1.9.1-(m-tolylcarbamoyl)cyclopropane-1-carboxylic acid (**2I**). White solid (75%), ^{1}H NMR (400 MHz, DMSO-d_6) δ 13.14 (s, 1H), 10.58 (s, 1H), 7.52 – 7.31 (m, 2H), 7.17 (t, *J* = 7.8 Hz, 1H), 6.87 (d, *J* = 7.4 Hz, 1H), 2.27 (s, 3H), 1.42 (s, 4H).

4.1.1.10.1-(p-tolylcarbamoyl)cyclopropane-1-carboxylic acid (**2J**). White solid (79%), ^{1}H NMR (400 MHz, DMSO-d_6) δ 13.11 (s, 1H), 10.54 (s, 1H), 7.60 – 7.36 (m, 2H), 7.20 – 6.99 (m, 2H), 2.25 (s, 3H), 1.42 (s, 4H).

4.1.1.11.1-((4-chloro-3-(trifluoromethyl)phenyl)carbamoyl)cyclopropane-1-carboxylic acid (**2K**). White solid (67%), ^{1}H NMR (400 MHz, DMSO-d_6) δ 13.13 (s, 1H),

10.88 (s, 1H), 8.20 (d, *J* = 2.3 Hz, 1H), 7.85 (d, *J* = 8.8 Hz, 1H), 7.71 – 7.43 (m, 1H), 1.42 (s, 4H); ^{13}C NMR (101 MHz, DMSO) δ 173.24, 167.32, 138.23, 131.95, 131.91, 126.82, 126.51, 124.01, 121.28, 117.97, 117.91, 29.02, 16.75.

4.1.2. General Procedure for the Preparation of **3A-K**.

To a two-necked flask, compound **2A-K** (30 mmol), *p*-Phenylenediamine (60 mmol), EDCI (45 mmol), HOBt (36 mmol), DIEA (60 mmol) and DMF (30 mL) were charged. The mixture was stirred at room temperature for 12 hours, then quenched by water. The mixture was extracted by ethyl acetate, and the combined organic layers were washed by saturated aqueous $NaHCO_3$ solution, water and brine, dried by anhydrous magnesium sulphate. The solvent was evaporated, and the residue was purified by silica gel column chromatography.

4.1.2.1. N-(4-aminophenyl)-N-(3-fluorophenyl)cyclopropane-1,1-dicarboxamide (**3A**). Brown solid (39%), ^{1}H NMR (400 MHz, DMSO-d_6) δ 10.47 (s, 1H), 9.47 (s, 1H), 7.69-7.58 (m, 1H), 7.40 -7.25 (m, 2H), 7.18 (d, *J* = 8.5 Hz, 2H), 6.88 (td, *J* = 7.8, 6.4, 2.1 Hz, 1H), 6.50 (d, *J* = 8.5 Hz, 2H), 4.91 (s, 2H), 1.53 -1.35 (m, 4H); ^{13}C NMR (101 MHz, DMSO) δ 169.07, 168.25, 162.47 (d, *J* = 240.8 Hz), 145.82, 141.06 (d, *J* = 11.2 Hz), 130.55 (d, *J* = 9.3 Hz), 127.84, 123.22, 116.25, 113.97, 110.33 (d, *J* = 21.4 Hz), 107.39 (d, *J* = 26.3 Hz), 31.38, 16.02.

4.1.2.2. N-(4-aminophenyl)-N-(4-fluorophenyl)cyclopropane-1,1-dicarboxamide (**3B**). Brown solid (54%), ^{1}H NMR (400 MHz, DMSO-d_6) δ 10.26 (s, 1H), 9.57 (s, 1H), 7.62 (dd, *J* = 8.9, 5.1 Hz, 2H), 7.20 (d, *J* = 8.3 Hz, 2H), 7.14 (t, *J* = 8.8 Hz, 2H), 6.51

(d, *J* = 8.4 Hz, 2H), 4.91 (s, 2H), 1.44 (d, *J* = 4.4 Hz, 4H); ^{13}C NMR (101 MHz, DMSO) δ 168.97, 168.33, 158.71 (d, *J* = 240.0 Hz), 145.80, 135.56, 127.91, 123.11, 122.71 (d, *J* = 7.9 Hz), 115.53 (d, *J* = 22.1 Hz), 114.03, 31.01, 16.05 .

4.1.2.3.N-(4-aminophenyl)-N-(3-chlorophenyl)cyclopropane-1,1-dicarboxamide (**3C**). Brown solid (58%), ^{1}H NMR (400 MHz, DMSO-d_6) δ 10.42 (s, 1H), 9.50 (s, 1H), 7.85 (t, *J* = 2.1 Hz, 1H), 7.49 (dd, *J* = 8.1, 1.9 Hz, 1H), 7.32 (t, *J* = 8.1 Hz, 1H), 7.26 -7.16 (m, 2H), 7.11 (dd, *J* = 7.9, 2.1 Hz, 1H), 6.55-6.44 (m, 2H), 4.91 (s, 2H), 1.52-1.38 (m, 4H); ^{13}C NMR (101 MHz, DMSO) δ 169.14, 168.14, 145.80, 140.78, 133.30, 130.63, 127.90, 123.59, 123.18, 120.21, 118.98, 113.99, 31.43, 16.02.

4.1.2.4. N-(4-aminophenyl)-N-(4-chlorophenyl)cyclopropane-1,1-dicarboxamide (**3D**). Brown solid (62%), ^{1}H NMR (400 MHz, DMSO-d_6) δ 10.39 (s, 1H), 9.52 (s, 1H), 7.65 (d, *J* = 8.6 Hz, 2H), 7.39-7.32 (m, 2H), 7.20 (d, *J* = 8.4 Hz, 2H), 6.51 (d, *J* = 8.5 Hz, 2H), 4.91 (s, 2H), 1.55 -1.38 (m, 4H); ^{13}C NMR (101 MHz, DMSO) δ 169.01, 168.30, 145.80, 138.23, 128.86, 127.88, 127.56, 123.17, 122.27, 114.01, 31.23, 16.08.

4.1.2.5.N-(4-aminophenyl)-N-(3-bromophenyl)cyclopropane-1,1-dicarboxamide (**3E**). Brown solid (58%), ^{1}H NMR (400 MHz, DMSO-d_6) δ 10.41 (s, 1H), 9.51 (s, 1H), 8.00 (s, 1H), 7.64 -7.38 (m, 1H), 7.37-7.09 (m, 4H), 6.52 (d, *J* = 8.2 Hz, 2H), 4.95 (s, 2H), 1.45 (d, *J* = 8.6 Hz, 4H). ^{13}C NMR (101 MHz, DMSO) δ 168.66, 167.67, 145.23, 140.41, 130.44, 127.47, 126.02, 122.69, 122.61, 121.31, 118.89, 113.57, 30.90, 15.58.

4.1.2.6.N-(4-aminophenyl)-N-(4-bromophenyl)cyclopropane-1,1-dicarboxamide (**3F**). Brown solid (62%), ^{1}H NMR (400 MHz, DMSO-d_6) δ 10.38 (s, 1H), 9.50 (s, 1H), 7.60 (d, *J* = 8.5 Hz, 2H), 7.48 (d, *J* = 8.4 Hz, 2H), 7.19 (d, *J* = 8.2 Hz, 2H), 6.50 (d, *J*

= 8.2 Hz, 2H), 4.92 (s, 2H), 1.44 (d, *J* = 7.1 Hz, 4H). ^{13}C NMR (101 MHz, DMSO) δ 168.52, 167.81, 145.31, 138.16, 131.29, 127.38, 122.68, 122.15, 115.12, 113.53, 30.77, 15.59.

4.1.2.7.N-(4-aminophenyl)-N-(3-(trifluoromethyl)phenyl)cyclopropane-1,1-dicarboxamide (**3G**). Brown solid (78%), ^{1}H NMR (400 MHz, DMSO-d_6) δ 10.50 (s, 1H), 9.73 (s, 1H), 8.16 (s, 1H), 7.83 (d, *J* = 8.2 Hz, 1H), 7.53 (t, *J* = 8.2 Hz, 1H), 7.39 (d, *J* = 7.7 Hz, 1H), 7.22 (d, *J* = 8.2 Hz, 2H), 6.52 (d, *J* = 8.2 Hz, 2H), 4.91 (s, 2H), 1.59 -1.35 (m, 4H); ^{13}C NMR (101 MHz, DMSO) δ 168.94, 167.58, 145.22, 139.96, 129.59, 129.19 (d, *J* = 31.1 Hz), 127.57, 123.73, 125.65 – 120.14 (m), 122.54, 119.51, 116.42 (d, *J* = 4.3 Hz), 113.52, 31.01, 15.49.

4.1.2.8.N-(4-aminophenyl)-N-(4-(trifluoromethyl)phenyl)cyclopropane-1,1-dicarboxamide (**3H**). Brown solid (50%), ^{1}H NMR (400 MHz, DMSO-d_6) δ 10.64 (s, 1H), 9.46 (s, 1H), 7.84 (d, *J* = 8.4 Hz, 2H), 7.66 (d, *J* = 8.4 Hz, 2H), 7.19 (d, *J* = 8.3 Hz, 2H), 6.50 (d, *J* = 8.3 Hz, 2H), 4.93 (s, 2H), 1.45 (d, *J* = 8.8 Hz, 4H); ^{13}C NMR (101 MHz, DMSO) δ 168.78, 167.68, 145.31, 142.45, 127.36, 125.90–125.57 (m), 122.73, 119.91, 113.48, 31.04, 15.59.

4.1.2.9.N-(4-aminophenyl)-N-(m-tolyl)cyclopropane-1,1-dicarboxamide (**3I**). Brown solid (83%), ^{1}H NMR (400 MHz, DMSO-d_6) δ 10.31 (s, 1H), 9.58 (s, 1H), 7.48 -7.37 (m, 2H), 7.20 (dd, *J* = 8.0, 5.2 Hz, 3H), 6.88 (d, *J* = 7.5 Hz, 1H), 6.52 (d, *J* = 8.3 Hz, 2H), 4.93 (s, 2H), 2.27 (s, 3H), 1.47 (d, *J* = 6.4 Hz, 4H); ^{13}C NMR (101 MHz, DMSO) δ 168.89, 168.77, 145.84, 139.03, 138.22, 128.87, 127.77, 124.73, 123.23, 121.27, 117.87, 114.04, 30.80, 21.59, 16.24.

4.1.2.10.N-(4-aminophenyl)-N-(p-tolyl)cyclopropane-1,1-dicarboxamide (**3J**). Brown solid (47%), ^{1}H NMR (400 MHz, DMSO-d_6) δ 10.19 (s, 1H), 9.56 (s, 1H), 7.48 (dd, *J* = 8.1, 5.0 Hz, 2H), 7.21-7.14 (m, 2H), 7.10 (d, *J* = 8.2 Hz, 2H), 6.60 – 6.45 (m, 2H), 4.92 (s, 2H), 2.25 (s, 3H), 1.51-1.40 (m, 4H); ^{13}C NMR (101 MHz, DMSO) δ 168.79, 168.63, 145.83, 136.59, 132.99, 129.39, 127.78, 123.13, 120.80, 114.00, 30.75, 20.92, 16.16.

4.1.2.11.N-(4-aminophenyl)-N-(4-chloro-3-(trifluoromethyl)phenyl)cyclopropane-1,1-dicarboxamide (**3K**). Yellow solid (29%), ^{1}H NMR (400 MHz, DMSO-d_6) δ 10.62 (s, 1H), 9.54 (s, 1H), 8.26 (d, *J* = 2.5 Hz, 1H), 7.89 (dd, *J* = 8.9, 2.5 Hz, 1H), 7.63 (d, *J* = 8.9 Hz, 1H), 7.21 (d, *J* = 8.7 Hz, 2H), 6.51 (d, *J* = 8.6 Hz, 2H), 5.26 (s, 2H), 1.44 (d, *J* = 7.3 Hz, 4H); ^{13}C NMR (101 MHz, DMSO) δ 169.40, 167.70, 145.70, 138.92, 132.44, 132.22, 128.07, 127.09, 126.78, 125.31, 124.59, 124.47, 123.06, 121.88, 119.41, 114.02, 31.78, 15.90.

4.1.3.General Procedure for the Preparation of **4D,4F,4H,4J,4K**.

To a two-necked flask, compound **2D,2F,2H,2J,2K**(30 mmol), 4-(aminomethyl)aniline dihydrochloride (30 mmol), EDCI (45 mmol), HOBt (36 mmol), DIEA (120 mmol) and DMF (30 mL) were charged. The mixture was stirred at room temperature for 12 hours, then quenched by water. The mixture was extracted by ethyl acetate, and the combined organic layers were washed by saturated aqueous $NaHCO_3$ solution, water and brine, dried by anhydrous magnesium sulphate. The solvent was evaporated, and the residue was purified by silica gel column

chromatography.

4.1.3.1.N-(4-aminobenzyl)-N-(4-chlorophenyl)cyclopropane-1,1-dicarboxamide (**4D**). Brown solid (70%). ^{1}H NMR (400 MHz, DMSO-d_6) δ 10.79 (s, 1H), 8.27 (d, *J* = 5.9 Hz, 1H), 7.63 (d, *J* = 8.4 Hz, 2H), 7.35 (d, *J* = 8.4 Hz, 2H), 6.93 (d, *J* = 8.0 Hz, 2H), 6.50 (d, *J* = 7.9 Hz, 2H), 4.96 (s, 2H), 4.15 (d, *J* = 5.8 Hz, 2H), 1.38 (d, *J* = 4.6 Hz, 4H). ^{13}C NMR (101 MHz, DMSO) δ 170.17, 168.34, 147.47, 137.62, 128.45, 128.15, 127.02, 126.08, 121.46, 113.68, 42.35, 29.43, 15.88.

4.1.3.2.N-(4-aminobenzyl)-N-(4-bromophenyl)cyclopropane-1,1-dicarboxamide (**4F**). Brown solid (55%). ^{1}H NMR (400 MHz, DMSO-d_6) δ 10.80 (s, 1H), 8.28 (t, *J* = 5.8 Hz, 1H), 7.58 (d, *J* = 8.6 Hz, 2H), 7.47 (d, *J* = 8.5 Hz, 2H), 6.93 (d, *J* = 7.9 Hz, 2H), 6.50 (d, *J* = 7.9 Hz, 2H), 4.95 (s, 2H), 4.15 (d, *J* = 5.6 Hz, 2H), 1.38 (d, *J* = 4.7 Hz, 4H). ^{13}C NMR (101 MHz, DMSO) δ 170.18, 168.35, 147.49, 138.03, 131.36, 128.16, 126.07, 121.82, 115.05, 113.67, 42.35, 29.44, 15.92.

4.1.3.3.N-(4-aminobenzyl)-N-(4-(trifluoromethyl)phenyl)cyclopropane-1,1-dicarboxamide (**4H**). Brown solid (70%). ^{1}H NMR (400 MHz, DMSO-d_6) δ 11.08 (s, 1H), 8.28 (d, *J* = 5.9 Hz, 1H), 7.83 (d, *J* = 8.4 Hz, 2H), 7.66 (d, *J* = 8.4 Hz, 2H), 6.93 (d, *J* = 7.9 Hz, 2H), 6.51 (d, *J* = 7.9 Hz, 2H), 4.95 (s, 2H), 4.16 (d, *J* = 5.6 Hz, 2H), 1.41 (d, *J* = 3.2 Hz, 4H). ^{13}C NMR (101 MHz, DMSO) δ 170.12, 168.71, 147.50, 142.27, 128.16, 126.06, 125.84 (d, *J* = 3.6 Hz), 124.62 (d, *J* = 213.2 Hz), 123.12 (d, *J* = 26.2 Hz), 119.68, 113.66, 42.37, 29.63, 16.02.

4.1.3.4.N-(4-aminobenzyl)-N-(p-tolyl)cyclopropane-1,1-dicarboxamide (**4J**). Brown solid (69%). ^{1}H NMR (400 MHz, DMSO-d_6) δ 10.67 (s, 1H), 8.29 (d, *J* = 5.9 Hz, 1H),

7.46 (dd, *J* = 8.2, 2.1 Hz, 2H), 7.10 (d, *J* = 7.9 Hz, 2H), 6.94 (d, *J* = 7.8 Hz, 2H), 6.52 (dd, *J* = 8.2, 2.2 Hz, 2H), 4.97 (s, 2H), 4.16 (d, *J* = 5.5 Hz, 2H), 2.25 (s, 3H), 1.40 (dd, *J* = 10.4, 2.7 Hz, 4H). ^{13}C NMR (101 MHz, DMSO) δ 170.56, 168.04, 147.48, 136.05, 132.45, 129.00, 128.16, 126.09, 119.92, 113.71, 42.32, 28.94, 20.41, 16.01.

4.1.3.5.N-(4-aminobenzyl)-N-(4-chloro-3-(trifluoromethyl)phenyl)cyclopropane-1,1-dicarboxamide (**4K**). Brown solid (80%). ^{1}H NMR (400 MHz, DMSO-d_6) δ 10.94 (s, 1H), 8.31 (t, *J* = 5.9 Hz, 1H), 8.25 (d, *J* = 2.3 Hz, 1H), 7.85 (dd, *J* = 8.8, 2.3 Hz, 1H), 7.63 (d, *J* = 8.7 Hz, 1H), 6.93 (d, *J* = 7.9 Hz, 2H), 6.50 (d, *J* = 7.9 Hz, 2H), 4.95 (s, 2H), 4.15 (d, *J* = 5.7 Hz, 2H), 1.38 (s, 4H).^{13}C NMR (101 MHz, DMSO) δ 169.59, 168.83, 147.49, 138.28, 131.79, 128.15, 126.52 (d, *J* = 30.6 Hz), 126.09, 124.62, 123.99, 122.73 (d, *J* = 272.8 Hz), 118.63 (d, *J* = 5.7 Hz), 113.64, 42.39, 30.03, 15.65.

4.1.4.General Procedure for the Preparation of **5A-K, 6D,6F,6H,6J,6K.**

To a suspension of 6-(2-chloro-5-fluoropyrimidin-4-yl)-4-fluoro-1-isopropyl-2-methyl-1H-benzo[d]imidazole (**7**) (645.48 mg, 2 mmol) in 20 mL 1,4-dioxane were added compound **3A-K**, **4D,4F,4H,4J,4K**(2 mmol), $Pd(OAc)_2$ (11 mg, 0.05 mmol), BINAP (62 mg, 0.1 mmol) and Cs_2CO_3 (978 mg, 3 mmol) and the flask was purged with Ar. Then the flask was sealed and the mixture was heated for 12 h at 100□. The reaction was cooled to rt, the solvent was removed under reduced pressure, and the residue was purified by silica gel column chromatography to obtain **5A-K**, **6D,6F,6H,6J,6K**.

4.1.4.1.N-(4-((5-fluoro-4-(4-fluoro-1-isopropyl-2-methyl-1H-benzo[d]imidazol-6-yl)pyrimidin-2-yl)amino)phenyl)-N-(3-fluorophenyl)cyclopropane-1,1-dicarboxamide(**5A**

). Light yellow solid, Yield(55%), Mp 227 □.^{1}H NMR (400 MHz, DMSO-d_6) δ 10.35 (s, 1H), 9.89 (s, 1H), 9.74 (s, 1H), 8.59 (dd, *J* = 3.9, 1.2 Hz, 1H), 8.25 (d, *J* = 1.3 Hz, 1H), 7.74 (d, *J* = 9.0 Hz, 2H), 7.68- 7.61 (m, 2H), 7.57 (d, *J* = 8.9 Hz, 2H), 7.43-7.29 (m, 2H), 6.94 -6.82 (m, 1H), 4.82 (p, *J* = 6.9 Hz, 1H), 2.63 (s, 3H), 1.62 (d, *J* = 6.9 Hz, 6H), 1.48 (d, *J* = 6.8 Hz, 4H). ^{13}C NMR (101 MHz, DMSO) δ 168.98, 168.26, 162.48 (d, *J* = 241.3 Hz), 156.79, 154.92, 153.99, 151.59 (d, *J* = 13.7 Hz), 150.25, 149.15, 148.24 (d, *J* = 26.8 Hz), 141.15 (d, *J* = 11.2 Hz), 136.96, 136.77 (d, *J* = 9.9 Hz), 133.62 (d, *J* = 16.6 Hz), 133.30, 130.52 (d, *J* = 8.9 Hz), 127.27 (t, *J* = 6.2 Hz), 121.47, 119.20, 116.38, 110.36 (d, *J* = 21.1 Hz), 109.21 (d, *J* = 6.9 Hz), 107.51 (d, *J* = 26.2 Hz), 48.57, 32.04, 21.40, 15.94, 14.99. ^{19}F NMR (376 MHz, DMSO-d_6) δ -107.69(s, 1F), -124.01(s, 1F), -146.01(s, 1F). ESI-HRMS m/z calcd for Chemical Formula: $C_{32}H_{29}F_3N_7O_2^+$ 600.2329, found 600.2323 $[M + H]^+$. HPLC purity 99%.

4.1.4.2.N-(4-((5-fluoro-4-(4-fluoro-1-isopropyl-2-methyl-1H-benzo[d]imidazol-6-yl)pyrimidin-2-yl)amino)phenyl)-N-(4-fluorophenyl)cyclopropane-1,1-dicarboxamide(**5B**). Light yellow solid, Yield(45%), Mp 140 □. ^{1}H NMR (400 MHz, DMSO-d_6) δ 10.12 (s, 1H), 9.98 (s, 1H), 9.73 (s, 1H), 8.64 – 8.55 (m, 1H), 8.25 (d, *J* = 1.3 Hz, 1H), 7.73 (d, *J* = 9.0 Hz, 2H), 7.68 – 7.61 (m, 3H), 7.57 (d, *J* = 8.7 Hz, 2H), 7.15 (t, *J* = 8.9 Hz, 2H), 4.83 (p, *J* = 6.9 Hz, 1H), 2.63 (s, 3H), 1.62 (d, *J* = 6.8 Hz, 6H), 1.51 – 1.42 (m, 4H). ^{13}C NMR (101 MHz, DMSO) δ 168.88, 168.34, 158.75 (d, *J* = 239.8 Hz), 156.81, 154.94, 154.00, 151.59 (d, *J* = 14.0 Hz), 150.27, 149.16, 148.24 (d, *J* = 26.2 Hz), 136.92, 136.78 (d, *J* = 9.8 Hz), 133.62 (d, *J* = 16.5 Hz), 133.32, 127.27 (t, *J* = 6.6 Hz), 122.85 (d, *J* = 7.8 Hz), 121.36, 119.25, 115.50 (d, *J* = 22.4 Hz), 109.25, 107.42 (dd, *J*

= 20.1, 8.1 Hz), 48.57, 31.65, 21.41, 15.96, 15.00. ^{19}F NMR (376 MHz, DMSO-d_6) δ -114.26(s, 1F), -124.04(s, 1F), -145.87(s, 1F).ESI-HRMS m/z calcd for Chemical Formula: $C_{32}H_{29}F_3N_7O_2^+$ 600.2329, found 600.2322 $[M + H]^+$. HPLC purity 100%.

4.1.4.3.N-(3-chlorophenyl)-N-(4-((5-fluoro-4-(4-fluoro-1-isopropyl-2-methyl-1H-benzo[d]imidazol-6-yl)pyrimidin-2-yl)amino)phenyl)cyclopropane-1,1-dicarboxamide (**5C**). Light yellow solid, Yield(51%), Mp 155 □. ^{1}H NMR (400 MHz, DMSO-d_6) δ 10.29 (s, 1H), 9.90 (s, 1H), 9.73 (s, 1H), 8.60 (d, *J* = 3.9 Hz, 1H), 8.25 (d, *J* = 1.3 Hz, 1H), 7.86 (t, *J* = 2.1 Hz, 1H), 7.73 (d, *J* = 9.0 Hz, 2H), 7.65 (dd, *J* = 11.9, 1.2 Hz, 1H), 7.60 – 7.50 (m, 3H), 7.33 (t, *J* = 8.1 Hz, 1H), 7.12 (ddd, *J* = 8.0, 2.1, 0.9 Hz, 1H), 4.83 (p, *J* = 6.9 Hz, 1H), 2.63 (s, 3H), 1.62 (d, *J* = 6.9 Hz, 6H), 1.47 (d, *J* = 6.0 Hz, 4H). ^{13}C NMR (101 MHz, DMSO) δ 169.02, 168.16, 156.81, 154.94, 154.00, 151.60 (d, *J* = 14.4 Hz), 150.29, 149.16, 148.26 (d, *J* = 27.8 Hz), 140.86, 136.94, 136.79 (d, *J* = 9.8 Hz), 133.62 (d, *J* = 16.6 Hz), 133.34, 130.61, 127.31 (d, *J* = 6.3 Hz), 123.63, 121.44 , 120.33, 119.23, 119.09, 109.26, 107.43 (dd, *J* = 20.1, 8.2 Hz), 48.58, 32.06, 21.41, 15.92, 15.01. ^{19}F NMR (376 MHz, DMSO-d_6) δ -123.91 (s, 1F) , -145.72 (s, 1F).ESI-HRMS m/z calcd for Chemical Formula: $C_{32}H_{29}ClF_2N_7O_2^+$ 616.2034, found 616.2033 $[M + H]^+$. HPLC purity 100%.

4.1.4.4.N-(4-chlorophenyl)-N-(4-((5-fluoro-4-(4-fluoro-1-isopropyl-2-methyl-1H-benzo[d]imidazol-6-yl)pyrimidin-2-yl)amino)phenyl)cyclopropane-1,1-dicarboxamide (**5D**). Light yellow solid, Yield(57%), Mp 245 □. ^{1}H NMR (400 MHz, DMSO-d_6) δ 10.22 (s, 1H), 9.90 (s, 1H), 9.73 (s, 1H), 8.61 (d, *J* = 3.8 Hz, 1H), 8.31 – 8.16 (m, 1H), 7.75 – 7.70 (m, 2H), 7.69 – 7.62 (m, 3H), 7.56 (d, *J* = 8.6 Hz, 2H), 7.36 (d, *J* = 8.9 Hz,

2H), 4.83 (p, *J* = 6.9 Hz, 1H), 2.63 (s, 3H), 1.61 (d, *J* = 6.9 Hz, 6H), 1.46 (d, *J* = 4.3 Hz, 4H). ^{13}C NMR (101 MHz, DMSO) δ 168.40, 167.78, 156.33, 154.46, 153.50, 151.10 (d, *J* = 14.1 Hz), 149.83, 148.67, 147.77 (d, *J* = 28.3 Hz), 136.43, 136.29 (d, *J* = 10.1 Hz), 133.12 (d, *J* = 16.7 Hz), 132.83, 128.35, 127.11, 126.78 (t, *J* = 6.6 Hz), 121.90, 120.92, 118.75, 108.76, 106.93 (d, *J* = 12.0 Hz), 48.08, 31.42, 20.92, 15.43, 14.52. ^{19}F NMR (376 MHz, DMSO-d_6) δ -124.04 (s, 1F), -145.95(s, 1F). ESI-HRMS m/z calcd for Chemical Formula: $C_{32}H_{29}ClF_2N_7O_2^+$ 616.2034, found 616.2030 $[M + H]^+$. HPLC purity 100%.

4.1.4.5.N-(3-bromophenyl)-N-(4-((5-fluoro-4-(4-fluoro-1-isopropyl-2-methyl-1H-benzo[d]imidazol-6-yl)pyrimidin-2-yl)amino)phenyl)cyclopropane-1,1-dicarboxamide (**5E**). Light yellow solid, Yield(43%), Mp 201 □. ^{1}H NMR (400 MHz, DMSO-d_6) δ 10.26 (s, 1H), 9.89 (s, 1H), 9.73 (s, 1H), 8.62 (d, *J* = 3.9 Hz, 1H), 8.25 (d, *J* = 1.4 Hz, 1H), 8.00 (d, *J* = 2.3 Hz, 1H), 7.73 (d, *J* = 9.0 Hz, 2H), 7.68 – 7.62 (m, 1H), 7.58 – 7.54 (m, 3H), 7.31 – 7.19 (m, 2H), 4.83 (p, *J* = 6.9 Hz, 1H), 2.64 (s, 3H), 1.62 (d, *J* = 6.8 Hz, 6H), 1.46 (d, *J* = 5.7 Hz, 4H).^{13}C NMR (101 MHz, DMSO) δ 168.50, 167.63, 156.32, 154.46, 153.50, 151.10 (d, *J* = 14.2 Hz), 149.84, 148.67, 147.78 (d, *J* = 26.6 Hz), 140.50, 136.42, 136.29 (d, *J* = 9.8 Hz), 133.12 (d, *J* = 16.8 Hz), 132.86, 130.44, 126.78 (t, *J* = 6.3 Hz), 126.03, 122.70, 121.24, 119.96 (d, *J* = 195.3 Hz), 118.74, 108.75, 107.34 – 106.13 (m), 48.08, 31.58, 20.92, 15.40, 14.52. ^{19}F NMR (376 MHz, DMSO-d_6) δ -123.94(s, 1F), -145.99 (s, 1F). ESI-HRMS m/z calcd for Chemical Formula: $C_{32}H_{29}BrF_2N_7O_2^+$ 660.1529, found 660.1530 $[M + H]^+$. HPLC purity 97%.

4.1.4.6.N-(4-bromophenyl)-N-(4-((5-fluoro-4-(4-fluoro-1-isopropyl-2-methyl-1H-benzo[d]imidazol-6-yl)pyrimidin-2-yl)amino)phenyl)cyclopropane-1,1-dicarboxamide (**5F**). Light yellow solid, Yield(46%), Mp 149.3 □. ^{1}H NMR (400 MHz, DMSO-d_6) δ 10.24 (s, 1H), 9.91 (s, 1H), 9.74 (s, 1H), 8.61 (d, *J* = 3.8 Hz, 1H), 8.27 – 8.18 (m, 1H), 7.72 (d, *J* = 8.9 Hz, 2H), 7.67 – 7.59 (m, 3H), 7.56 (d, *J* = 8.7 Hz, 2H), 7.51 – 7.44 (m, 2H), 4.82 (p, *J* = 6.9 Hz, 1H), 2.63 (s, 3H), 1.61 (d, *J* = 6.9 Hz, 6H), 1.46 (q, *J* = 3.4 Hz, 4H).^{13}C NMR (101 MHz, DMSO) δ 168.88, 168.25, 156.81, 154.95, 153.99, 151.59 (d, *J* = 14.6 Hz), 150.26, 149.16, 148.27 (d, *J* = 25.7 Hz), 136.91, 136.77 (d, *J* = 10.0 Hz), 133.61 (d, *J* = 16.9 Hz), 133.33, 131.76, 127.27 (t, *J* = 6.6 Hz), 122.74, 121.39, 119.22, 115.64, 109.24, 107.70-106.86 (m), 48.57, 31.97, 21.41, 15.93, 15.02. ^{19}F NMR (376 MHz, DMSO-d_6) δ -123.95 (s, 1F), -145.98 (s, 1F). ESI-HRMS m/z calcd for Chemical Formula: $C_{32}H_{29}BrF_2N_7O_2^+$ 660.1529, found 660.1522 $[M + H]^+$. HPLC purity 95%.

4.1.4.7.N-(4-((5-fluoro-4-(4-fluoro-1-isopropyl-2-methyl-1H-benzo[d]imidazol-6-yl)pyrimidin-2-yl)amino)phenyl)-N-(3-(trifluoromethyl)phenyl)cyclopropane-1,1-dicarboxamide (**5G**). Light yellow solid, Yield(47%), Mp 158 □.^{1}H NMR (400 MHz, DMSO-d_6) δ 10.42 (s, 1H), 9.91 (s, 1H), 9.73 (s, 1H), 8.61 (d, *J* = 3.8 Hz, 1H), 8.25 (s, 1H), 8.16 (s, 1H), 7.85 (d, *J* = 8.3 Hz, 1H), 7.73 (d, *J* = 9.0 Hz, 2H), 7.65 (d, *J* = 12.1 Hz, 1H), 7.55 (dd, *J* = 15.6, 8.2 Hz, 3H), 7.41 (d, *J* = 7.7 Hz, 1H), 4.82 (p, *J* = 6.9 Hz, 1H), 2.63 (s, 3H), 1.61 (d, *J* = 6.9 Hz, 6H), 1.48 (t, *J* = 3.0 Hz, 4H). ^{13}C NMR (101 MHz, DMSO) δ 168.70, 167.52, 156.33, 154.44, 153.50, 151.10 (d, *J* = 14.1 Hz), 149.79, 148.67, 147.77 (d, *J* = 26.2 Hz), 139.72, 136.41, 136.29 (d, *J* = 9.8 Hz),

133.12 (d, *J* = 16.4 Hz), 132.91, 129.65, 129.18 (d, *J* = 30.8 Hz), 126.78 (t, *J* = 6.4 Hz), 124.14 (d, *J* = 272.4 Hz), 120.88, 119.71 (d, *J* = 4.4 Hz), 118.74, 116.47 (d, *J* = 4.4 Hz), 108.74, 107.35-106.13 (m), 48.07, 31.71, 20.90, 15.35, 14.50. ^{19}F NMR (376 MHz, DMSO-d_6) δ -56.49(s, 3F), -123.96 (s, 1F), -146.00 (s, 1F). ESI-HRMS m/z calcd for Chemical Formula: $C_{33}H_{29}F_5N_7O_2^+$ 650.2297, found 650.2295 $[M + H]^+$. HPLC purity 100%.

4.1.4.8.N-(4-((5-fluoro-4-(4-fluoro-1-isopropyl-2-methyl-1H-benzo[d]imidazol-6-yl)pyrimidin-2-yl)amino)phenyl)-N-(4-(trifluoromethyl)phenyl)cyclopropane-1,1-dicarboxamide (**5H**). Light yellow solid, Yield(51%), Mp 149 □. ^{1}H NMR (400 MHz, DMSO-d_6) δ 10.51 (s, 1H), 9.88 (s, 1H), 9.74 (s, 1H), 8.61 (d, *J* = 3.9 Hz, 1H), 8.25 (d, *J* = 1.3 Hz, 1H), 7.87 (d, *J* = 8.5 Hz, 2H), 7.76 – 7.70 (m, 2H), 7.67 (dd, *J* = 10.5, 8.7 Hz, 3H), 7.57 (d, *J* = 8.9 Hz, 2H), 4.82 (p, *J* = 6.9 Hz, 1H), 2.63 (s, 3H), 1.61 (d, *J* = 6.9 Hz, 6H), 1.51-1.46 (m, 4H). ^{13}C NMR (101 MHz, DMSO) δ 168.68, 167.70, 156.31 (d, *J* = 1.8 Hz), 154.43, 153.50, 151.10 (d, *J* = 14.1 Hz), 149.76, 148.67, 147.76 (d, *J* = 26.7 Hz), 142.55, 136.45, 136.29 (d, *J* = 9.8 Hz), 133.12 (d, *J* = 17.2 Hz), 132.83, 126.78 (t, *J* = 6.6 Hz), 125.73 (d, *J* = 3.6 Hz), 123.62 -122.84 (m), 120.97, 120.02, 118.73, 108.74 (d, J = 6.6 Hz), 106.92 (dd, J = 19.9, 8.4 Hz), 48.07, 31.70, 20.90, 15.48, 14.49. ^{19}F NMR (376 MHz, DMSO-d_6) δ -55.52 (s, 3F), -124.05 (s, 1F), -145.93 (s, 1F). ESI-HRMS m/z calcd for Chemical Formula: $C_{33}H_{29}F_5N_7O_2^+$ 650.2297, found 650.2300 $[M + H]^+$. HPLC purity100%.

4.1.4.9.N-(4-((5-fluoro-4-(4-fluoro-1-isopropyl-2-methyl-1H-benzo[d]imidazol-6-yl)pyrimidin-2-yl)amino)phenyl)-N-(m-tolyl)cyclopropane-1,1-dicarboxamide (**5I**). Light

yellow solid, Yield(40%), Mp 188 □. ^{1}H NMR (400 MHz, DMSO-d_6) δ 10.09 (s, 1H), 9.94 (s, 1H), 9.75 (s, 1H), 8.63 – 8.55 (m, 1H), 8.25 (d, *J* = 1.3 Hz, 1H), 7.74 (d, *J* = 9.0 Hz, 2H), 7.65 (dd, *J* = 11.9, 1.3 Hz, 1H), 7.59 – 7.54 (m, 2H), 7.47 – 7.39 (m, 2H), 7.19 (t, *J* = 7.8 Hz, 1H), 6.91 – 6.84 (m, 1H), 4.83 (p, *J* = 6.9 Hz, 1H), 2.63 (s, 3H), 2.28 (s, 3H), 1.62 (d, *J* = 6.9 Hz, 6H), 1.48 (d, *J* = 4.0 Hz, 4H).^{13}C NMR (101 MHz, DMSO) δ 168.78, 168.67, 156.80, 154.95, 154.00, 151.60 (d, *J* = 14.7 Hz), 150.28, 149.16, 148.25 (d, *J* = 28.6 Hz), 139.13, 138.14, 136.97, 136.78 (d, *J* = 9.7 Hz), 133.62 (d, *J* = 17.3 Hz), 133.22, 128.82, 127.62 -126.53 (m), 124.75, 121.45 (d, *J* = 5.1 Hz), 119.23, 118.04, 109.26, 107.47 (d, *J* = 19.9 Hz), 48.57, 31.51, 21.59, 21.41, 16.09, 15.00. ^{19}F NMR (376 MHz, DMSO-d_6) δ -124.03 (s, 1F), -145.92 (s, 1F). ESI-HRMS m/z calcd for Chemical Formula: $C_{33}H_{32}F_2N_7O_2^+$ 596.2580, found 596.2580 $[M + H]^+$. HPLC purity 100%.

4.1.4.10.N-(4-((5-fluoro-4-(4-fluoro-1-isopropyl-2-methyl-1H-benzo[d]imidazol-6-yl) pyrimidin-2-yl)amino)phenyl)-N-(p-tolyl)cyclopropane-1,1-dicarboxamide (**5J**). Light yellow solid, Yield(60%), Mp 147.1 □. ^{1}H NMR (400 MHz, DMSO-d_6) δ 10.02 (s, 1H), 9.98 (s, 1H), 9.74 (s, 1H), 8.60 (d, *J* = 3.9 Hz, 1H), 8.25 (d, *J* = 1.3 Hz, 1H), 7.76 - 7.70 (m, 2H), 7.65 (dd, *J* = 11.9, 1.2 Hz, 1H), 7.59 -7.53 (m, 2H), 7.52 -7.44 (m, 2H), 7.11 (d, *J* = 8.2 Hz, 2H), 4.83 (p, *J* = 6.9 Hz, 1H), 2.63 (s, 3H), 2.25 (s, 3H), 1.62 (d, *J* = 6.9 Hz, 6H), 1.54-1.35 (m, 4H). ^{13}C NMR (101 MHz, DMSO) δ 168.76, 168.64, 156.81, 154.94, 154.00, 151.60 (d, *J* = 14.0 Hz), 150.27, 149.17, 148.25 (d, *J* = 26.7 Hz), 136.95, 136.79 (d, *J* = 9.9 Hz), 136.65, 133.63 (d, *J* = 17.3 Hz), 133.15 (d, *J* = 19.5 Hz), 129.36, 127.28 (t, *J* = 6.5 Hz), 121.42, 121.00, 119.27, 109.24 (d, *J* = 6.6

Hz), 107.43 (dd, *J* = 20.1, 8.2 Hz), 48.58, 31.42, 21.41, 20.91, 16.07, 15.01. ^{19}F NMR (376 MHz, DMSO-d_6) δ -123.95 (s, 1F), -145.98 (s, 1F). ESI-HRMS m/z calcd for Chemical Formula: $C_{33}H_{32}F_2N_7O_2^+$ 596.2580, found 596.2579 $[M + H]^+$. HPLC purity 100%.

4.1.4.11.N-(4-chloro-3-(trifluoromethyl)phenyl)-N-(4-((5-fluoro-4-(4-fluoro-1-isopropyl-2-methyl-1H-benzo[d]imidazol-6-yl)pyrimidin-2-yl)amino)phenyl)cyclopropane-1,1-dicarboxamide (**5K**). Light yellow solid, Yield(53%), Mp 158 □. ^{1}H NMR (400 MHz, DMSO-d_6) δ 10.51 (d, *J* = 3.2 Hz, 1H), 9.92 (d, *J* = 2.6 Hz, 1H), 9.73 (s, 1H), 8.60 (d, *J* = 3.7 Hz, 1H), 8.26 (dd, *J* = 9.1, 1.9 Hz, 2H), 7.91 (dd, *J* = 8.8, 2.6 Hz, 1H), 7.72 (d, *J* = 8.8 Hz, 2H), 7.65 (dd, *J* = 10.3, 2.9 Hz, 2H), 7.57 (d, *J* = 9.0 Hz, 2H), 4.81 (p, *J* = 6.9 Hz, 1H), 2.63 (s, 3H), 1.61 (d, *J* = 6.8 Hz, 6H), 1.46 (d, *J* = 5.5 Hz, 4H).^{13}C NMR (101 MHz, DMSO) δ 168.75, 167.26, 156.29, 154.41, 153.50, 151.09 (d, *J* = 14.0 Hz), 149.71, 148.66, 147.75 (d, *J* = 27.1 Hz), 138.50, 136.41, 136.22, 133.12 (d, *J* = 17.2 Hz), 132.93, 131.76, 126.78 (d, *J* = 12.1 Hz), 124.89, 124.02, 122.76 (d, *J* = 273.0 Hz), 120.81, 118.98 (d, *J* = 6.0 Hz), 118.74, 108.70, 106.92 (dd, *J* = 20.1, 8.3 Hz), 48.07, 31.86, 20.89, 15.32, 14.48. ^{19}F NMR (376 MHz, DMSO-d_6) δ -56.71(s, 3F), -123.93 (s, 1F), -145.97 (s, 1F). ESI-HRMS m/z calcd for Chemical Formula: $C_{33}H_{28}ClF_5N_7O_2^+$ 684.1908, found 684.1913 $[M + H]^+$. HPLC purity 100%.

4.1.4.12.N-(4-chlorophenyl)-N-(4-((5-fluoro-4-(4-fluoro-1-isopropyl-2-methyl-1H-benzo[d]imidazol-6-yl)pyrimidin-2-yl)amino)benzyl)cyclopropane-1,1-dicarboxamide (**6D**). Light yellow solid, Yield(49%), Mp 238 □. ^{1}H NMR (400 MHz, DMSO-d_6) δ

10.80 (d, *J* = 2.6 Hz, 1H), 9.75 (s, 1H), 8.70 – 8.55 (m, 1H), 8.44 (s, 1H), 8.24 (d, *J* = 1.3 Hz, 1H), 7.74 (d, *J* = 8.5 Hz, 2H), 7.66 – 7.58 (m, 3H), 7.33 (d, *J* = 8.9 Hz, 2H), 7.20 (d, *J* = 8.4 Hz, 2H), 4.95 – 4.62 (m, 1H), 4.29 (d, *J* = 5.8 Hz, 2H), 2.61 (s, 3H), 1.60 (d, *J* = 6.9 Hz, 6H), 1.41 (t, *J* = 2.9 Hz, 4H). ^{13}C NMR (101 MHz, DMSO) δ 170.93, 168.75, 156.77, 154.92, 153.98, 151.61 (d, *J* = 19.6 Hz), 150.31, 149.20, 148.27 (d, *J* = 26.3 Hz), 139.78, 138.12, 136.77 (d, *J* = 10.3 Hz), 133.63 (d, *J* = 17.0 Hz), 132.79, 128.94, 127.93, 127.54, 127.25 (t, *J* = 6.5 Hz), 121.94, 119.02 , 109.17 (d, *J* = 5.4 Hz), 107.47 (dd, *J* = 20.1, 8.4 Hz), 48.57, 42.76, 30.02, 21.38, 16.43, 14.98. ^{19}F NMR (376 MHz, DMSO-d_6) δ -123.92 (s, 1F), -145.70 (s, 1F). ESI-HRMS m/z calcd for Chemical Formula: $C_{33}H_{31}ClF_2N_7O_2^+$ 630.2190, found 630.2183 $[M + H]^+$. HPLC purity 98%.

4.1.4.13.N-(4-bromophenyl)-N-(4-((5-fluoro-4-(4-fluoro-1-isopropyl-2-methyl-1H-benzo[d]imidazol-6-yl)pyrimidin-2-yl)amino)benzyl)cyclopropane-1,1-dicarboxamide (**6F**). Light yellow solid, Yield(45%), Mp 240 □.Yield(45%).^{1}H NMR (400 MHz, DMSO-d_6) δ 10.82 (s, 1H), 9.76 (s, H), 8.61 (d, *J* = 3.9 Hz, 1H), 8.45 (t, *J* = 5.8 Hz, 1H), 8.25 (d, *J* = 1.3 Hz, 1H), 7.75 (d, *J* = 8.4 Hz, 2H), 7.65 (dd, *J* = 11.9, 1.2 Hz, 1H), 7.59 (d, *J* = 8.9 Hz, 2H), 7.47 (d, *J* = 8.9 Hz, 2H), 7.22 (d, *J* = 8.5 Hz, 2H), 4.79 (p, *J* = 6.9 Hz, 1H), 4.30 (d, *J* = 5.8 Hz, 2H), 2.62 (s, 3H), 1.61 (d, *J* = 6.8 Hz,6H), 1.42 (d, *J* = 2.8 Hz, 4H). ^{13}C NMR (101 MHz, DMSO) δ 170.92, 168.75, 156.78, 154.93, 153.98, 151.61 (d, *J* = 19.6 Hz), 150.32, 149.20, 148.28 (d, *J* = 26.3 Hz), 139.78, 138.55, 136.77 (d, *J* = 9.8 Hz), 133.63 (d, *J* = 16.5 Hz), 132.79, 131.86, 127.93, 127.25 (t, *J* = 6.7 Hz), 122.31, 119.02, 115.56, 109.22, 107.47 (dd, *J* = 20.1, 8.4 Hz),

48.57, 42.75, 30.05, 21.38, 16.44, 15.00. ^{19}F NMR (376 MHz, DMSO-d_6) δ -123.93 (s, 1F), -145.72 (s, 1F). ESI-HRMS m/z calcd for Chemical Formula: $C_{33}H_{31}BrF_2N_7O_2^+$ 674.1685, found 674.1681 $[M + H]^+$. HPLC purity 95%.

4.1.4.14.N-(4-((5-fluoro-4-(4-fluoro-1-isopropyl-2-methyl-1H-benzo[d]imidazol-6-yl) pyrimidin-2-yl)amino)benzyl)-N-(4-(trifluoromethyl)phenyl)cyclopropane-1,1-dicarbo xamide (**6H**). Light yellow solid, Yield(64%), Mp 241 □. ^{1}H NMR (400 MHz, DMSO-d_6) δ 11.10 (s, 1H), 9.78 (s, 1H), 8.61 (d, *J* = 3.8 Hz, 1H), 8.47 (t, *J* = 5.9 Hz, 1H), 8.25 (d, *J* = 1.3 Hz, 1H), 7.84 (d, *J* = 8.5 Hz, 2H), 7.75 (d, *J* = 8.4 Hz, 2H), 7.69 – 7.59 (m, 3H), 7.22 (d, *J* = 8.3 Hz, 2H), 4.79 (p, *J* = 6.9 Hz, 1H), 4.30 (d, *J* = 5.7 Hz, 2H), 2.61 (s, 3H), 1.61 (d, *J* = 6.9 Hz, 6H), 1.44 (s, 4H). ^{13}C NMR (101 MHz, DMSO) δ 170.85, 169.10, 156.77, 154.92, 153.98, 151.61 (d, *J* = 19.2 Hz), 150.32, 149.19, 148.27 (d, *J* = 26.6 Hz), 142.78, 139.79, 136.76 (d, *J* = 9.7 Hz), 133.62 (d, *J* = 17.0 Hz), 132.78, 127.94, 127.50 – 127.12 (m), 126.33 (t, *J* = 4.0 Hz), 125.11 (d, *J* = 213.7 Hz), 123.60 (d, *J* = 25.6 Hz), 120.16, 119.00, 109.15, 107.46 (dd, *J* = 20.1, 8.5 Hz), 48.57, 42.76, 30.27, 21.36, 16.54, 14.96. ^{19}F NMR (376 MHz, DMSO-d_6) δ -55.58(s, 3F), -123.98 (s, 1F), -145.77 (s, 1F). ESI-HRMS m/z calcd for Chemical Formula: $C_{34}H_{31}F_5N_7O_2^+$ 664.2454, found 664.2451 $[M + H]^+$. HPLC purity 97%.

4.1.4.15.N-(4-((5-fluoro-4-(4-fluoro-1-isopropyl-2-methyl-1H-benzo[d]imidazol-6-yl) pyrimidin-2-yl)amino)benzyl)-N-(p-tolyl)cyclopropane-1,1-dicarboxamide (**6J**). Light yellow solid, Yield(56%), Mp 232 □. ^{1}H NMR (400 MHz, DMSO-d_6) δ 10.68 (s, 1H), 9.77 (s, 1H), 8.60 (d, *J* = 3.9 Hz, 1H), 8.46 (t, *J* = 5.9 Hz, 1H), 8.25 (d, *J* = 1.3 Hz,

1H), 7.87 – 7.70 (m, 2H), 7.65 (dd, *J* = 11.9, 1.2 Hz, 1H), 7.51 – 7.38 (m, 2H), 7.25 – 7.15 (m, 2H), 7.15 – 7.02 (m, 2H), 4.76 (p, *J* = 6.9 Hz, 1H), 4.30 (d, *J* = 5.8 Hz, 2H), 2.61 (s, 3H), 2.23 (s, 3H), 1.60 (d, *J* = 6.9 Hz, 6H), 1.42 (d, *J* = 7.8 Hz, 4H). ^{13}C NMR (101 MHz, DMSO) δ 171.32, 168.41, 156.77, 154.92, 153.97, 151.60 (d, *J* = 20.4 Hz), 150.21 (d, *J* = 7.8 Hz), 149.20, 148.31 (d, *J* = 27.0 Hz), 139.79, 136.75 (d, *J* = 9.0 Hz), 136.56, 133.63 (d, *J* = 16.5 Hz), 132.94, 132.79, 129.48, 127.91, 127.25 (t, *J* = 6.6 Hz), 120.38, 119.02, 109.18, 107.49 (dd, *J* = 20.2, 8.7 Hz), 48.57, 42.71, 29.52, 21.36, 20.89, 16.54, 14.96. ^{19}F NMR (376 MHz, DMSO-d_6) δ -124.00 (s, 1F), -145.74 (s, 1F). ESI-HRMS m/z calcd for Chemical Formula: $C_{34}H_{34}F_2N_7O_2^+$ 610.2737, found 610.2733 $[M + H]^+$. HPLC purity 97%.

4.1.4.16.N-(4-chloro-3-(trifluoromethyl)phenyl)-N-(4-((5-fluoro-4-(4-fluoro-1-isopropyl-2-methyl-1H-benzo[d]imidazol-6-yl)pyrimidin-2-yl)amino)benzyl)cyclopropane-1,1-dicarboxamide (**6K**). Light yellow solid, Yield(66%), Mp 243 □. ^{1}H NMR (400 MHz, DMSO-d_6) δ 10.95 (s, 1H), 9.76 (s, 1H), 8.60 (d, *J* = 1.1 Hz, 1H), 8.49 (t, *J* = 5.9 Hz, 1H), 8.25 (dd, *J* = 7.0, 2.0 Hz, 2H), 7.85 (dd, *J* = 8.8, 2.6 Hz, 1H), 7.79 – 7.69 (m, 2H), 7.68 – 7.57 (m, 2H), 7.21 (d, *J* = 8.5 Hz, 2H), 4.80 (p, *J* = 6.9 Hz, 1H), 4.30 (d, *J* = 5.7 Hz, 2H), 2.62 (s, 3H), 1.61 (d, *J* = 6.9 Hz, 6H), 1.41 (s, 4H). ^{13}C NMR (101 MHz, DMSO) δ 170.33, 169.23, 156.77, 154.91, 153.98, 151.60 (d, *J* = 18.7 Hz), 150.31, 149.19, 148.24 (d, *J* = 25.9 Hz), 139.78, 138.79, 136.76 (d, *J* = 9.9 Hz), 133.62 (d, *J* = 17.3 Hz), 132.82, 132.30, 127.93, 127.32 – 127.09 (m), 126.99 (d, *J* = 92.1 Hz), 126.84, 125.09, 124.53 (d, *J* = 7.3 Hz), 121.86, 118.99, 109.18, 107.46 (dd, *J* = 20.3, 8.3 Hz), 48.57, 42.80, 30.66, 21.36, 16.18, 14.96. ^{19}F NMR (376 MHz,

DMSO-d_6) δ -56.76(s, 1F), -123.95 (s, 1F), -145.74 (s, 1F). ESI-HRMS m/z calcd for Chemical Formula: $C_{34}H_{30}ClF_5N_7O_2^+$ 698.2064, found 698.2059 $[M + H]^+$. HPLC purity 98%.

*4.1.5.Synthesis of intermediate compound **13.***

4.1.5.1.5-bromo-N-isopropyl-2-nitroaniline(**9**). An orange mixture of 4-bromo-2-fluoro-1 –nitrobenzene **8** (4 g, 18.18 mmol), isopropylamine (1.7 mL, 20 mmol) and K_2CO_3 (2.51 g, 36.36 mmol) in DMF (40 mL) was stirred at room temperature overnight. The resulting mixture was diluted with water and the mixture was extracted by ethyl acetate, and the combined organic layers were washed by water and brine, dried by anhydrous magnesium sulphate. The solvent was evaporated, and the residue was purified by silica gel column chromatography to obtain **9** (4.52 g, 96%) as a bright orange solid. ^{1}H NMR (400 MHz, DMSO-d_6) δ 8.08 -7.77 (m, 2H), 7.20 (d, *J* = 2.5 Hz, 1H), 6.76 (dd, *J* = 9.1, 2.3 Hz, 1H), 4.08 -3.77 (m, 1H), 1.23 (dd, *J* = 6.4, 2.3 Hz, 6H). ^{13}C NMR (101 MHz, DMSO) δ 145.12, 131.60, 130.47, 128.55, 118.48, 117.14, 44.09, 22.51.

4.1.5.2.5-bromo-N^1-isopropylbenzene-1,2-diamine(**10**). Compound **2** (4 g, 15.4 mmol) was dissolved in AcOH (100 mL) and Fe powder (8.6 g, 154 mmol, 10 equiv) was added. The mixture was stirred at r.t. for 0.5 h and then heated at 70 °C for 3 h. The suspension was basified with aq$NaHCO_3$, diluted with CH_2Cl_2 (150 mL), and filtered through celite. The filtrate was extracted with CH_2Cl_2 (2 × 100 mL) and the combined organic phases were dried (K_2CO_3) and evaporated to furnish **10** (3.2 g, 91%) as a dark solid. The crude product **10** is not subjected to further purification and is taken directly.

4.1.5.3. 6-bromo-1-isopropyl-1H-benzo[d][1,2,3]triazole(**11**). To a 0 °C mixture of the crude product **10** (3.2 g, 14 mmol) in conc.HCl(40 mL) was added $NaNO_2$(1.1g,15.4 mmol) in H_2O(10 mL). The mixture was allowed to warm to room

temperature and stirred for 1 h. After recooling to 0 °C, the mixture was treated with 6N NaOH until basic, the precipitate filtered, rinsed with H_2O and dried to afford **11**(2.62 g, 78%). ^{1}H NMR (400 MHz, DMSO-d_6) δ 8.27 (d, *J* = 2.4 Hz, 1H), 7.98 (dd, *J* = 8.9, 2.3 Hz, 1H), 7.48 (dq, *J* = 8.8, 1.6 Hz, 1H), 5.21 (td, *J* = 6.7, 2.3 Hz, 1H), 1.59 (dd, *J* = 6.8, 2.4 Hz, 6H). ^{13}C NMR (101 MHz, DMSO) δ 147.32, 132.32, 129.26, 119.05, 117.79, 84.53, 83.27, 51.07, 25.27, 25.14, 22.75.

4.1.5.4.1-isopropyl-6-(4,4,5,5-tetramethyl-1,3,2-dioxaborolan-2-yl)-1H benzo[d][1,2,3]triazole(**12**). To a suspension of compound (**11**) (3 g, 12.5 mmol) in 50 mL 1,4-dioxane were added bis(pinacolato)diboron (3.81 g, 15 mmol 1.2 equiv), $PdCl_2$(pddf) (457 mg, 0.625 mmol, 0.05 equiv) and KOAc (4.3 g, 43.8 mmol, 3.5 equiv) and the flask was purged with N_2. Then the flask was sealed and the mixture was heated for 12 h at 95□. The reaction was cooled to r.t, the solvent was removed under reduced pressure, and the residue was purified by silica gel column chromatography to obtain **12** (2.4 g, 67%).^{1}H NMR (400 MHz, DMSO-d_6) δ 8.17 (s, 1H), 8.01 (d, *J* = 8.3 Hz, 1H), 7.64 (d, *J* = 8.4 Hz, 1H), 5.33 (p, *J* = 6.7 Hz, 1H), 1.61 (d, *J* = 6.7 Hz, 6H), 1.32 (s, 12 H).^{13}C NMR (101 MHz, DMSO) δ 147.32, 132.32, 129.26, 119.05, 117.79, 83.27, 51.07, 25.14, 22.75.

4.1.5.5.6-(2-chloro-5-fluoropyrimidin-4-yl)-1-isopropyl-1H-benzo[d][1,2,3]triazole (**13**). To a suspension of compound (**12**) (2 g, 7 mmol) in 50 mL 1,4-dioxane and 5 mL H_2O were added 2,4-dichloro-5-fluoropyrimidine (2.3 g, 14 mmol , 2 equiv), $PdCl_2$(pddf) (512 mg, 0.7 mmol, 0.1 equiv) and $NaHCO_3$ (1.8 g, 21 mmol, 3 equiv) and the flask was purged with N_2. Then the flask was sealed and the mixture was heated for 12 h at 100□. The reaction was cooled to r.t, the solvent was removed under reduced pressure, and the residue was purified by silica gel column chromatography to obtain **13** (1.2 g, 59%).^{1}H NMR (400 MHz, DMSO-d_6) δ 8.98 (d, *J* = 3.0 Hz, 1H), 8.46 (s, 1H), 8.16 (d, *J* = 8.7 Hz, 1H), 8.03 – 7.82 (m, 1H), 5.34 (p, *J* = 6.7 Hz, 1H), 1.64 (d, *J* = 6.6 Hz, 6H). ^{13}C NMR (101 MHz, DMSO) δ 155.49 (d, *J* = 265.4 Hz), 154.70 (d, *J* = 3.6 Hz), 153.95 (d, *J* = 10.1 Hz), 150.48 (d, *J* = 26.8 Hz), 146.76, 132.36, 130.17 (d, *J* = 5.1 Hz), 124.57 (d, *J* = 5.8 Hz), 120.16, 112.80 (d, *J* =

7.3 Hz), 51.58, 22.57.

4.1.6.General Procedure for the Preparation of **14A-K.**

To a suspension of 6-(2-chloro-5-fluoropyrimidin-4-yl)-1-isopropyl-1H-benzo[d][1,2,3]triazole (**6**) (583.4 mg, 2 mmol) in 20 mL 1,4-dioxane were added compound **3A-K** (2 mmol), $Pd(OAc)_2$ (11 mg, 0.05 mmol), BINAP (62 mg, 0.1 mmol) and Cs_2CO_3 (978 mg, 3 mmol) and the flask was purged with Ar. Then the flask was sealed and the mixture was heated for 12 h at 100□. The reaction was cooled to rt, the solvent was removed under reduced pressure, and the residue was purified by silica gel column chromatography to obtain **14A-K**.

4.1.6.1.N-(4-((5-fluoro-4-(1-isopropyl-1H-benzo[d][1,2,3]triazol-6-yl)pyrimidin-2-yl) amino)phenyl)-N-(3-fluorophenyl)cyclopropane-1,1-dicarboxamide (**14A**). Light yellow solid, Yield(65%), Mp 230 □.Solid. ^{1}H NMR (400 MHz, DMSO-d_6) δ 10.34 (s, 1H), 9.88 (s, 1H), 9.83 (s, 1H), 8.68 (d, *J* = 3.4 Hz, 1H), 8.51 (s, 1H), 8.22 (d, *J* = 8.8 Hz, 1H), 8.03 (dt, *J* = 8.8, 1.3 Hz, 1H), 7.73 (d, *J* = 8.8 Hz, 2H), 7.64 (dt, *J* = 11.9, 2.2 Hz, 1H), 7.55 (d, *J* = 8.7 Hz, 2H), 7.43 – 7.26 (m, 2H), 6.96 – 6.76 (m, 1H), 5.32 (p, *J* = 6.7 Hz, 1H), 1.68 (d, *J* = 6.7 Hz, 6H), 1.49 – 1.41 (m, 4H). ^{13}C NMR (101 MHz, DMSO-d_6) δ 168.98, 168.30, 162.47 (d, J = 240.7 Hz), 156.98 (d, J = 2.2 Hz), 151.75, 151.02 (d, J = 8.7 Hz), 149.24, 148.26 (d, J = 25.7 Hz), 146.62, 141.13 (d, J = 11.0 Hz), 136.87, 132.80 (d, J = 99.5 Hz), 132.36, 130.54 (d, J = 9.4 Hz), 124.69 (d, J = 5.4 Hz), 121.60, 120.00, 119.22, 116.37, 112.25 (d, J = 7.0 Hz), 110.37 (d, J = 21.0 Hz), 107.51 (d, J = 26.3 Hz), 51.76, 31.99, 22.50, 15.95. ^{19}F NMR (376 MHz, DMSO-d_6) δ -107.54 (s, 1F), -146.01 (s, 1F). ESI-HRMS m/z calcd for Chemical Formula: $C_{30}H_{27}F_2N_8O_2^+$ 569.2220, found 569.2216 $[M + H]^+$. HPLC purity 99%.

4.1.6.2.N-(4-((5-fluoro-4-(1-isopropyl-1H-benzo[d][1,2,3]triazol-6-yl)pyrimidin-2-yl) amino)phenyl)-N-(4-fluorophenyl)cyclopropane-1,1-dicarboxamide (**14B**). Light yellow solid, Yield(48%), Mp 249 □. ^{1}H NMR (400 MHz, DMSO-d_6) δ 10.05 (d, *J* =

48.6 Hz, 2H), 9.82 (s, 1H), 8.67 (d, *J* = 3.2 Hz, 1H), 8.51 (s, 1H), 8.22 (d, *J* = 8.7 Hz, 1H), 8.02 (dd, *J* = 8.8, 1.3 Hz, 1H), 7.75–7.69 (m, 2H), 7.67–7.60 (m, 2H), 7.55 (d, *J* = 8.9 Hz, 2H), 7.14 (t, *J* = 8.9 Hz, 2H), 5.32 (p, *J* = 6.7 Hz, 1H), 1.68 (d, *J* = 6.7 Hz, 6H), 1.47 (d, *J* = 1.6 Hz, 4H). ^{13}C NMR (101 MHz, DMSO-d_6) δ 168.89, 168.38, 158.73 (d, *J* = 240.0 Hz), 156.99 (d, *J* = 2.1 Hz), 151.74, 151.01 (d, *J* = 9.0 Hz), 149.23, 148.25 (d, *J* = 26.2 Hz), 146.63, 136.83, 135.62 (d, *J* = 2.0 Hz), 133.32, 132.36, 132.31, 124.69 (d, *J* = 5.7 Hz), 122.85 (d, *J* = 8.3 Hz), 121.48, 119.99, 119.25, 115.50 (d, *J* = 21.4 Hz), 112.24 (d, *J* = 6.7 Hz), 51.76, 31.56, 22.50, 16.01. ^{19}F NMR (376 MHz, DMSO-d_6) δ -114.14 (s, 1F), -146.03 (s, 1F). ESI-HRMS m/z calcd for Chemical Formula: $C_{30}H_{27}F_2N_8O_2^+$ 569.2220, found 569.2213 $[M + H]^+$. HPLC purity100%.

4.1.6.3.N-(3-chlorophenyl)-N-(4-((5-fluoro-4-(1-isopropyl-1H-benzo[d][1,2,3]triazol-6-yl)pyrimidin-2-yl)amino)phenyl)cyclopropane-1,1-dicarboxamide (**14C**). Light yellow solid, Yield(41%), Mp 227.1 □. ^{1}H NMR (400 MHz, DMSO-d_6) δ 10.29 (s, 1H), 9.89 (s, 1H), 9.82 (s, 1H), 8.67 (d, *J* = 3.5 Hz, 1H), 8.51 (s, 1H), 8.22 (d, *J* = 8.8 Hz, 1H), 8.03 (dt, *J* = 8.8, 1.4 Hz, 1H), 7.86 (d, *J* = 2.1 Hz, 1H), 7.76 – 7.68 (m, 2H), 7.60 – 7.44 (m, 3H), 7.32 (t, *J* = 8.0 Hz, 1H), 7.11 (dd, *J* = 7.9, 2.0 Hz, 1H), 5.32 (p, *J* = 6.7 Hz, 1H), 1.68 (d, *J* = 6.7 Hz, 6H), 1.47 (d, *J* = 5.1 Hz,4H). ^{13}C NMR (101 MHz, DMSO-d_6) δ 168.55, 167.71, 156.49 (d, *J* = 2.2 Hz), 151.25, 150.51 (d, *J* = 9.5 Hz), 148.74, 147.75 (d, *J* = 25.6 Hz), 146.13, 140.33, 136.37, 132.82, 132.80, 131.87, 131.81, 130.11, 124.18 (d, *J* = 5.5 Hz), 123.14, 121.07, 119.83, 119.50, 118.75, 118.59, 111.73 (d, *J* = 6.9 Hz), 51.27, 31.47, 22.00, 15.48. ^{19}F NMR (376 MHz, DMSO-d_6) δ -146.03 (s, 1F). ESI-HRMS m/z calcd for Chemical Formula: $C_{30}H_{27}ClFN_8O_2^+$ 585.1924, found 585.1918 $[M + H]^+$. HPLC purity 97%.

4.1.6.4.N-(4-chlorophenyl)-N-(4-((5-fluoro-4-(1-isopropyl-1H-benzo[d][1,2,3]triazol-6-yl)pyrimidin-2-yl)amino)phenyl)cyclopropane-1,1-dicarboxamide (**14D**). Light yellow solid, Yield(40%), Mp 271 □. ^{1}H NMR (400 MHz, DMSO-d_6) δ 10.23 (s, 1H), 9.92 (s, 1H), 9.81 (s, 1H), 8.67 (d, *J* = 3.3 Hz, 1H), 8.51 (d, *J* = 1.3 Hz, 1H), 8.22 (dd, *J* = 8.8, 0.8 Hz, 1H), 8.03 (dt, *J* = 8.7, 1.3 Hz, 1H), 7.73 (d, *J* = 9.0 Hz, 2H), 7.67 (d, *J*

= 8.9 Hz, 2H), 7.55 (d, *J* = 9.0 Hz, 2H), 7.35 (d, *J* = 8.9 Hz, 2H), 5.32 (p, *J* = 6.7 Hz, 1H), 1.68 (d, *J* = 6.7 Hz, 6H), 1.47 (d, *J* = 3.9 Hz, 4H). ^{13}C NMR (101 MHz, DMSO-d_6) δ 168.93, 168.35, 156.99 (d, *J* = 2.9 Hz), 151.75, 151.01 (d, *J* = 8.6 Hz), 149.24, 148.24 (d, *J* = 25.9 Hz), 146.64, 138.28, 136.88, 133.29, 132.37, 132.31, 128.84, 127.63, 124.68 (d, *J* = 5.5 Hz), 122.40, 121.55, 119.99, 119.25, 112.22 (d, *J* = 7.0 Hz), 51.76, 31.80, 22.49, 16.03.

^{19}F NMR (376 MHz, DMSO-d_6) δ -145.98 (s, 1F). ESI-HRMS m/z calcd for Chemical Formula: $C_{30}H_{27}ClFN_8O_2^+$ 585.1924, found 585.1918 $[M + H]^+$. HPLC purity 96%.

4.1.6.5.N-(3-bromophenyl)-N-(4-((5-fluoro-4-(1-isopropyl-1H-benzo[d][1,2,3]triazol-6-yl)pyrimidin-2-yl)amino)phenyl)cyclopropane-1,1-dicarboxamide (**14E**). Light yellow solid, Yield(62%), Mp 221 □. ^{1}H NMR (400 MHz, DMSO-d_6) δ 10.26 (s, 1H), 9.89 (s, 1H), 9.81 (s, 1H), 8.67 (d, *J* = 3.4 Hz, 1H), 8.51 (s, 1H), 8.22 (d, *J* = 8.8 Hz, 1H), 8.08 – 7.95 (m, 2H), 7.76 – 7.64 (m, 2H), 7.55 (dt, *J* = 6.5, 2.0 Hz, 3H), 7.29 – 7.15 (m, 2H), 5.32 (p, *J* = 6.7 Hz, 1H), 1.68 (d, *J* = 6.7 Hz, 6H), 1.54-1.33 (m, 4H). ^{13}C NMR (101 MHz, DMSO) δ 168.54, 167.69, 156.49 (d, *J* = 2.0 Hz), 151.25, 150.51 (d, *J* = 9.7 Hz), 148.75, 147.89, 147.63, 146.13, 140.47, 136.36, 132.83, 131.87, 131.81, 130.43, 126.03, 124.18 (d, *J* = 5.4 Hz), 122.70, 121.25, 121.05, 119.50, 118.98, 118.75, 111.74 (d, *J* = 7.2 Hz), 51.27, 31.48, 22.00, 15.47.
^{19}F NMR (376 MHz, DMSO-d_6) δ -146.01 (s, 1F). ESI-HRMS m/z calcd for Chemical Formula: $C_{30}H_{27}BrFN_8O_2^+$ 629.1419, found 629.1421 $[M + H]^+$. HPLC purity 98%.

4.1.6.6.N-(4-bromophenyl)-N-(4-((5-fluoro-4-(1-isopropyl-1H-benzo[d][1,2,3]triazol-6-yl)pyrimidin-2-yl)amino)phenyl)cyclopropane-1,1-dicarboxamide (**14F**). Light yellow solid, Yield(65%), Mp 271 □. ^{1}H NMR (400 MHz, DMSO-d_6) δ 10.24 (s, 1H), 9.91 (s, 1H), 9.82 (s, 1H), 8.68 (d, *J* = 3.4 Hz, 1H), 8.52 (d, *J* = 1.4 Hz, 1H), 8.23 (dd, *J* = 8.8, 0.7 Hz, 1H), 8.04 (dt, *J* = 8.8, 1.3 Hz, 1H), 7.73 (d, *J* = 9.0 Hz, 2H), 7.62 (d, *J* = 8.9 Hz, 2H), 7.56 (d, *J* = 9.0 Hz, 2H), 7.49 (d, *J* = 8.9 Hz, 2H), 5.33 (p, *J* = 6.7 Hz,

1H), 1.69 (d, *J* = 6.7 Hz, 6H), 1.48 (d, *J* = 3.8 Hz, 4H). ^{13}C NMR (101 MHz, DMSO-d_6) δ 168.92, 168.33, 156.99 (d, *J* = 2.1 Hz), 151.75, 151.03 (d, *J* = 8.7 Hz), 149.25, 148.25 (d, *J* = 25.9 Hz), 146.64, 138.72, 136.86, 133.30, 132.37, 132.31, 131.76, 124.68 (d, *J* = 5.4 Hz), 122.76, 121.55, 120.00, 119.24, 115.67, 112.24 (d, *J* = 6.7 Hz), 51.76, 31.86, 22.50, 16.00. ^{19}F NMR (376 MHz, DMSO-d_6) δ -146.02 (s, 1F). ESI-HRMS m/z calcd for Chemical Formula: $C_{30}H_{27}BrFN_8O_2^+$ 629.1419, found 629.1417 $[M + H]^+$. HPLC purity 95%.

4.1.6.7.N-(4-((5-fluoro-4-(1-isopropyl-1H-benzo[d][1,2,3]triazol-6-yl)pyrimidin-2-yl) amino)phenyl)-N-(3-(trifluoromethyl)phenyl)cyclopropane-1,1-dicarboxamide (**14G**). Light yellow solid, Yield(51%), Mp 252.7 □. ^{1}H NMR (400 MHz, DMSO-d_6) δ 10.42 (s, 1H), 9.92 (s, 1H), 9.82 (s, 1H), 8.68 (d, *J* = 3.3 Hz, 1H), 8.51 (s, 1H), 8.22 (d, *J* = 8.8 Hz, 1H), 8.16 (s, 1H), 8.05 – 8.01 (m, 1H), 7.85 (d, *J* = 8.2 Hz, 1H), 7.75 – 7.71 (m, 2H), 7.61 – 7.50 (m, 3H), 7.41 (d, *J* = 7.8 Hz, 1H), 5.32 (p, *J* = 6.7 Hz, 1H), 1.68 (d, *J* = 6.7 Hz, 6H), 1.48 (d, *J* = 2.0 Hz, 4H). ^{13}C NMR (101 MHz, DMSO) δ 168.73, 167.57, 156.49 (d, *J* = 2.3 Hz), 151.25, 150.50 (d, *J* = 9.2 Hz), 148.74, 147.75 (d, *J* = 25.6 Hz), 146.14, 139.70, 136.34, 132.89, 131.87, 131.82, 129.64, 129.19 (d, *J* = 32.0 Hz), 124.17 (d, *J* = 5.6 Hz), 123.74, 121.01, 119.71 (d, *J* = 4.5 Hz), 119.49, 118.75, 116.47 (d, *J* = 4.2 Hz), 111.73 (d, *J* = 7.2 Hz), 51.26, 31.61, 21.98, 15.41. ^{19}F NMR (376 MHz, DMSO-d_6) δ -55.43(s, 3F), -145.98 (s, 1F). ESI-HRMS m/z calcd for Chemical Formula: $C_{31}H_{27}F_4N_8O_2^+$ 619.2188, found 619.2183 $[M + H]^+$. HPLC purity 96%.

4.1.6.8.N-(4-((5-fluoro-4-(1-isopropyl-1H-benzo[d][1,2,3]triazol-6-yl)pyrimidin-2-yl) amino)phenyl)-N-(4-(trifluoromethyl)phenyl)cyclopropane-1,1-dicarboxamide (**14H**). Light yellow solid, Yield(50%), Mp 207 □. ^{1}H NMR (400 MHz, DMSO-d_6) δ 10.52 (s, 1H), 9.89 (s, 1H), 9.82 (s, 1H), 8.68 (d, *J* = 3.3 Hz, 1H), 8.51 (s, 1H), 8.23 (d, *J* = 8.7 Hz, 1H), 8.03 (d, *J* = 8.7 Hz, 1H), 7.87 (d, *J* = 8.3 Hz, 2H), 7.72 (d, *J* = 8.7 Hz, 2H), 7.67 (d, *J* = 8.5 Hz, 2H), 7.55 (d, *J* = 8.6 Hz, 2H), 5.32 (p, *J* = 6.7 Hz, 1H), 1.68 (d, *J* = 6.6 Hz, 6H), 1.48 (q, *J* = 3.2 Hz, 4H). ^{13}C NMR (101 MHz, DMSO-d_6) δ

168.71, 167.74, 156.49 (d, *J* = 2.0 Hz), 151.25, 150.55 (d, *J* = 10.1 Hz), 148.75, 147.78 (d, *J* = 24.3 Hz), 146.13, 142.56, 136.37, 132.83, 131.87, 131.81, 125.75 (d, *J* = 4.1 Hz), 124.19 (d, *J* = 5.4 Hz), 123.62 – 122.86 (m), 121.09, 120.02, 119.51, 118.72, 111.76 (d, *J* = 7.1 Hz), 51.26, 31.70, 22.00, 15.50. ^{19}F NMR (376 MHz, DMSO-d_6) δ -56.50(s, 3F), -146.03 (s, 1F). ESI-HRMS m/z calcd for Chemical Formula: $C_{31}H_{27}F_4N_8O_2^+$ 619.2188, found 619.2197 $[M + H]^+$. HPLC purity 99%.

4.1.6.9.N-(4-((5-fluoro-4-(1-isopropyl-1H-benzo[d][1,2,3]triazol-6-yl)pyrimidin-2-yl) amino)phenyl)-N-(m-tolyl)cyclopropane-1,1-dicarboxamide (**14I**). Light yellow solid, Yield(55%), Mp 161.1 □.^{1}H NMR (400 MHz, DMSO-d_6) δ 10.10 (s, 1H), 9.94 (s, 1H), 9.83 (s, 1H), 8.68 (dd, *J* = 3.5, 1.1 Hz, 1H), 8.51 (s, 1H), 8.23 (d, *J* = 8.8 Hz, 1H), 8.03 (dt, *J* = 8.8, 1.4 Hz, 1H), 7.82 – 7.68 (m, 2H), 7.62 – 7.49 (m, 2H), 7.49 – 7.37 (m, 2H), 7.18 (t, *J* = 7.8 Hz, 1H), 6.88 (d, *J* = 7.4 Hz, 1H), 5.32 (p, *J* = 6.7 Hz, 1H), 2.27 (s, 3H), 1.68 (d, *J* = 6.7 Hz, 6H), 1.49 (q, *J* = 3.3 Hz, 4H). ^{13}C NMR (101 MHz, DMSO) δ 168.81, 168.73, 156.99 (d, *J* = 1.8 Hz), 151.74, 151.00 (d, *J* = 5.5 Hz), 149.24, 148.25 (d, *J* = 26.5 Hz), 146.63, 139.10, 138.16, 136.91, 133.20, 132.36, 132.31, 128.82, 124.76, 124.72, 124.66, 121.52 (d, *J* = 18.5 Hz), 119.99, 119.24, 118.03, 112.23 (d, *J* = 7.1 Hz), 51.76, 31.40, 22.50, 21.59, 16.16. ^{19}F NMR (376 MHz, DMSO-d_6) δ -146.01 (s, 1F). ESI-HRMS m/z calcd for Chemical Formula: $C_{31}H_{30}FN_8O_2^+$ 565.2470, found 565.2467 $[M + H]^+$. HPLC purity 99%.

4.1.6.1.N-(4-((5-fluoro-4-(1-isopropyl-1H-benzo[d][1,2,3]triazol-6-yl)pyrimidin-2-yl) amino)phenyl)-N-(p-tolyl)cyclopropane-1,1-dicarboxamide (**14J**). Light yellow solid, Yield(56%), Mp 238 □. ^{1}H NMR (400 MHz, DMSO-d_6) δ 10.03 (s, 1H), 9.98 (s, 1H), 9.82 (s, 1H), 8.67 (d, *J* = 3.3 Hz, 1H), 8.51 (s, 1H), 8.22 (d, *J* = 8.7 Hz, 1H), 8.03 (dd, *J* = 8.7, 1.4 Hz, 1H), 7.76 – 7.70 (m, 2H), 7.55 (d, *J* = 9.0 Hz, 2H), 7.49 (d, *J* = 8.5 Hz, 2H), 7.10 (d, *J* = 8.2 Hz, 2H), 5.32 (p, *J* = 6.7 Hz, 1H), 2.24 (s, 3H), 1.68 (d, *J* = 6.7 Hz, 6H), 1.48 (s, 4H). ^{13}C NMR (101 MHz, DMSO) δ 168.29, 168.19, 156.49 (d, *J* = 2.4 Hz), 151.25, 150.50 (d, *J* = 8.3 Hz), 148.74, 147.73 (d, *J* = 25.2 Hz), 146.14, 136.39, 136.13, 132.72, 132.57, 131.87, 131.81, 128.86, 124.18 (d, *J* = 5.5 Hz),

121.04, 120.50, 119.49, 118.77, 111.72 (d, *J* = 6.8 Hz), 51.26, 30.80, 21.99, 20.41, 15.64. ^{19}F NMR (376 MHz, DMSO-d_6) δ -146.0 (s, 1F). ESI-HRMS m/z calcd for Chemical Formula: $C_{31}H_{30}FN_8O_2^+$ 565.2470, found 565.2469 $[M + H]^+$. HPLC purity 99%.

N-(4-chloro-3-(trifluoromethyl)phenyl)-N-(4-((5-fluoro-4-(1-isopropyl-1H-benzo[d][1,2,3]triazol-6-yl)pyrimidin-2-yl)amino)phenyl)cyclopropane-1,1-dicarboxamide (**14K**). Light yellow solid, Yield(44%), Mp 279 □. ^{1}H NMR (400 MHz, DMSO-d_6) δ 10.50 (s, 1H), 9.91 (s, 1H), 9.82 (s, 1H), 8.68 (d, *J* = 3.5 Hz, 1H), 8.51 (d, *J* = 1.3 Hz, 1H), 8.27 (d, *J* = 2.6 Hz, 1H), 8.23 (d, *J* = 8.8 Hz, 1H), 8.03 (dt, *J* = 8.8, 1.4 Hz, 1H), 7.90 (dd, *J* = 8.9, 2.5 Hz, 1H), 7.72 (d, *J* = 9.0 Hz, 2H), 7.66 (d, *J* = 8.8 Hz, 1H), 7.55 (d, *J* = 9.1 Hz, 2H), 5.32 (p, *J* = 6.7 Hz, 1H), 1.68 (d, *J* = 6.7 Hz, 6H), 1.46 (d, *J* = 4.2 Hz, 4H). ^{13}C NMR (101 MHz, DMSO) δ 168.76, 167.29, 156.49 (d, *J* = 2.5 Hz), 151.25, 150.48, 148.74, 147.78 (d, *J* = 25.5 Hz), 146.13, 138.50, 136.33, 132.93, 131.87, 131.81, 131.79, 126.42 (d, *J* = 30.5 Hz), 124.90, 124.18 (d, *J* = 5.5 Hz), 124.06 (d, *J* = 10.3 Hz), 121.40, 120.94, 119.51, 118.97 (d, *J* = 5.6 Hz), 118.74, 111.75 (d, *J* = 7.1 Hz), 51.25, 31.84, 21.99, 15.33. ^{19}F NMR (376 MHz, DMSO-d_6) δ -56.68(s, 3F), -146.06 (s, 1F). ESI-HRMS m/z calcd for Chemical Formula: $C_{31}H_{26}ClF_4N_8O_2^+$ 653.1798, found 653.1792 $[M + H]^+$. HPLC purity 95%.

4.1.2 **Procedure for Log P and Log D7.4 determination.** Log P and Log $D_{7.4}$ was determined by using well-known 'shake-flask' method and the concentrations of the test compound in the two phases were determined by HPLC (Shimadzu Prominence-i LC-2030C 3D system. column, InertSustain C_{18}, 4.6 mm × 250 mm, 5 μm; mobile phase, gradient elution of methanol/H_2O; low rate, 1.0 mL/min; UV wavelength, 190−800 nm; temperature, 40 °C; injection volume, 20 μL).

The Log P was calculated by employing the following equation:

Log P = log (C_{OCT}/C_{H2O}); C_{OCT}, C_{H2O} were the compound's concentration in two phases

Log $D_{7.4}$ = log (C_{OCT}/C_{PBS}); C_{OCT}, C_{PBS} were the compound's concentration in two phases

4.2 Biology

4.2.1. Cell culture

Human cancer cell lines were purchased from ATCC. All the cell lines were recently authenticated by cellular morphology and the short tandem repeat analysis at Microread Inc. (Beijing, China; May 2014) according to the guideline from ATCC. MDA-MB-231, T-47D, HeLa and A431 cells were maintained in DMEM medium, SiHa, MCF-7, A549, K562 and HUVEC cells were maintained in 1640 medium, UM1 cells were maintained in DMEM/F12 medium. All cell lines were supplemented with 10% fetal bovine serum (FBS) and 1% penicillin/streptomycin at 37°C with 5% CO_2.

4.2.2. IC_{50} calculation and cell viability assay

Cells (3×10^3 cells/well) growing in 96-well plates were respectively cultured with different concentrations of **Roxyl-ZV-5J**, cabozantinib, abemaciclib or vehicle. For IC_{50} calculation, cell viability was quantified according to the manufacturer's protocols of CCK-8 kit (DOJINDO Laboratories) after 72 h. For time-dependent cell viability assay, cell viability was measured at 0 h, 12 h, 24 h, 36 h, 48 h, 60 h and 72 h

using CCK-8 kit. The absorbance was measured at 450 nm using a microplate ELISA reader, with DMSO used as the blank. Five parallel replicates were measured for each sample.

4.2.3. Colony formation assay

MDA-MB-231, T-47D, SiHa and HeLa cells (4×10^3 cells/well) were seeded in 24-well plates and cultured with different concentrations of **Roxyl-ZV-5J**, cabozantinib, abemaciclib or vehicle. After 5 days, cells were fixed with 20% methanol, stained with 0.5% crystal violet and photographed under a light microscope (Olympus).

4.2.4. Flow cytometry

Cell cycle was detected by flow cytometry using a cell cycle analysis kit (BD Bioscience). MDA-MB-231, T-47D, SiHa and HeLa cells were treated with different concentrations of **Roxyl-ZV-5J**, cabozantinib, abemaciclib or vehicle for 36 h. Then, cells were harvested and fixed in 70% ice-cold ethanol at 4°C overnight, cells were centrifuged and resuspended by PBS, subsequently, stained with a solution containing 50 μg/ml PI and 5 μg/ml RNase at 37°C for 30 min. Cell cycle was analyzed by FACS using BD FACSDiva™ software v6.1.3 and BD CellQuest™ Pro (BD Biosciences).

Cell apoptosis was detected by flow cytometry using an FITC Annexin V Apoptosis Detection Kit-1 (BD Biosciences). MDA-MB-231, T-47D, SiHa and HeLa cells were treated with different concentrations of **Roxyl-ZV-5J**, cabozantinib, abemaciclib or vehicle for 48 h, the experimental protocol was performed as

described previously [36]. Subsequently, the cells were analyzed by flow cytometry, using BD FACSDiva™ software v6.1.3 and BD CellQuest™ Pro (BD Biosciences).

4.2.5. Tube formation assay

A pre-chilled 48-well plate was coated with 150 μl Matrigel (BD Bioscience) and solidified at 37°C for 30 min. HUVEC cells (4×10^4 cells/well) were seeded on the Matrigel and treated with different concentrations of **Roxyl-ZV-5J**, Cabozantinib or vehicle at 37°C for 6 h. After incubation, 3 randomly fields were counted and photographed under a light microscope (Olympus).

4.2.6. EdU proliferation assay

MDA-MB-231, T-47D, SiHa and HeLa cells (5×10^4) were seeded in 24-well plates and treated with different concentrations of **Roxyl-ZV-5J**, cabozantinib, abemaciclib or vehicle for 48 h, then, assayed with a Cell-Light™ EdU Apollo 488 In Vitro Imaging Kit according to the manufacturer's instructions (RiboBio). Slides were photographed using FV-1000 laser scanning confocal biological microscopy. Percentages of EdU –positive cells were calculated as follows: (EdU-positive cells/Hoechst stained cells) × 100%.

4.2.7. Western Blot assay

After treating with different concentrations of **Roxyl-ZV-5J**, cabozantinib, abemaciclib or vehicle for 48 h, MDA-MB-231, T-47D, SiHa, HeLa and HUVEC cells were washed three times with phosphate-buffered saline (PBS) and lysed in RIPA-buffer (EMD Millipore, Billerica, MA,USA). Preparation of total cell extracts

and immunoblotting with appropriate antibodies was performed as previously described [37]. The following primary antibodies were used: mouse anti-Rb (dilution, 1:1000; #9309, Cell Signaling Technology), rabbit anti-phospho-Rb (dilution, 1:1000; #8516, Cell Signaling Technology), rabbit anti-Ki67 (dilution, 1:1000; #GR259204-2, abcam), rabbit anti-Bcl-2 (dilution, 1:1000; #51-6511GR, BD Biosciences), goat anti-VEGFR2 (dilution,1:1000; #2479, Cell Signaling Technology), rabbit anti-phosphor-VEGFR2 (dilution,1:1000; #24798, Cell Signaling Technology), mouse anti-STAT3 (dilution, 1:1000; #sc-8019, Santa Cruz Biotechnology), mouse anti-phospho-STAT3 (dilution, 1:1000; #sc-8059, Santa Cruz Biotechnology), goat anti-Akt (dilution, 1:1000; #zs-16190, ZSGB-BIO), rabbit anti-phospho-Akt (dilution, 1:1000; #sc-16646-R, ZSGB-BIO), rabbit anti-Erk1 (dilution, 1:1000; #zs-940, ZSGB-BIO), rabbit anti-phospho-Erk1 (dilution, 1:1000; #zs-79760-R, ZSGB-BIO), rabbit anti-Src (dilution, 1:1000; #2109, Cell Signaling Technology), rabbit anti-p-Src (dilution, 1:1000; #12432, Cell Signaling Technology), mouse anti-β-actin (dilution, 1:1000; #sc-47778, Santa Cruz Biotechnology).

4.2.7. Matrigel plug assay

The experimental procedures of the animal study were proved by the Animal Care and Use Committee at Nankai University. 5 weeks old Balb/C mice were given subcutaneous injection of 750 μL of a 2:1 mixture of growth factor-reduced Matrigel (BD Biosciences) and **Roxyl-ZV-5J** (10 mg/kg, 20 mg/kg), cabozantinib (20 mg/kg) or vehicle. After 10 days, Balb/c mice were sacrificed and taken hypodermatomy. Then, the plugs were harvested and subcutaneous angiogenesis were photografted.

4.2.8. Tumor xenograft experiments

6 to 8 weeks old female Balb/c NOD/SCID mice were housed in a specific pathogen-free (SPF) animal facility. To implement subcutaneous human cervical tumors, 2×10^6 SiHa cells were dispensed in 100 μL medium and injected into the right flank of the mice. When tumors reached a volume of 100 mm^3, mice were randomly divided into six groups (5 mice/group) to have gavage administration with different doses of **Roxyl-ZV-5J**, cabozantinib, abemaciclib or vehicle once per day. Tumor volumes (*V*) were calculated by measuring the length (*L*) and width (*W*) of the tumor with calipers and using the following formula: $V= L \times W^2 /2$.

4.2.9. Hematoxylin and eosin (H&E) staining

H&E staining was performed on the formalin-fixed, paraffin-embedded xenograft mice tumor tissues. Tumor tissue sections were deparaffinized, counterstained with hematoxylin and eosin, then observed under a light microscopy (Olympus).

4.2.10. Immunohistochemistry staining

For immunohistochemistry assay, tumor tissue sections were deparaffinized, rehydrated and incubated with primary antibody of Ki67 (#GR259204-2, abcam) and CD31 (#3528, Cell Signaling Technology) diluted 1:100, at 4 °C overnight, then tissues were incubated with biotin-labeled secondary antibody (Vector Laboratories. Inc. Burlingame. CA) at room temperature for 1 h. Sections were incubated with ABC-peroxidase and diaminobenzidine (DAB), counterstaining with hematoxylin and

observed under a light microscopy (Olympus).

4.2.11. Acute toxicity assay

A total of 20 Balb/c mice (10 male and 10 female; 4-6 week, weight, 18-22 g) were purchased from Beijing HFK Bioscience CO., LTD. The mice were randomly divided into two groups (10 mice/group; male/female ratio, 1:1) and fasted with free access to water for the 12 h prior to the experiment. **Roxyl-ZV-5J** in DMSO was gavaged into the mice, while the control group was gavaged with an equal volume of normal solvent. Any signs of toxicity and behavioral abnormality were observed after the administration of the drug and whether any mice died during experimentation. Histological (the major organs) and hematological factors were evaluated.

For histological examination, Balb/c mice were treated with **Roxyl-ZV-5J** 40 mg/kg or negative control orally at 0 h, 24 h and 48 h. Following experimentation, the mice were sacrificed by cervical dislocation and two mice from each group were randomly selected for dissection to observe the color and shape of the gross specimen. The fatal organs, including heart, liver, spleen, lung, kidney and brain were excised after mice were sacrificed after 48 h. H&E staining were performed.

For hematological examination, mice were treated with **Roxyl-ZV-5J** 40 mg/kg or negative control orally once two days for 4 times and then sacrificed. The blood was taken from the inner canthus. Blood was examined using hematology analyzer (Celltac E, NIHON KOHDEN)

4.2.12. Assessments of Pharmacokinetic Properties [38]

The pharmacokinetics analysis of **5J** was conducted in male Sprague−Dawley rats (Chinese Academy of Medical Science, Beijing, China). Briefly, catheters were surgically placed into the jugular veins of the rats to collect serial blood samples. **5J** was dissolved in saline with 5% (v/v) DMSO. The animals were administered a single dose of 10 mg/kg **5J** by iv and po after fasting overnight. Blood was collected and centrifuged immediately to isolate plasma. The plasma concentrations were determined using high performance liquid chromatography with HPLC analysis on a Shimadzu Prominence-i LC-2030C 3D system and were identified by tandem mass spectrometric detection (3200 QTRAP system, Applied Biosystems). Noncompartmental pharmacokinetic parameters were fitted using DAS software (Enterprise, version 2.0, Mathematical Pharmacology Professional Committee of China).

4.2.13. Statistical Analysis

Statistical analysis of preliminary data was performed used GraphPad Prism 5.02. Data points represented the mean values ± SD and error bars represented standard deviations of three independent biological replicates. P-value<0.05 was considered to indicate a statistically significant difference.

4.2.14 Docking studies

Since there is no 3D structure of CDK4-ligand complex reported at present, the structure of CDK6 in complex with an inhibitor (PDB entry: 4EZ5) was used as a template for homology modeling. MODELLER [39] in the Discovery Studio

(Accelrys, San Diego, CA) (DS) was employed for the homology modeling. Then the compound **Roxyl-ZV-5J** was docked to CDK4 and VEGFR2 (PDB code: 2OH4) by GOLD (version 5.0). Hydrogen atoms were added to the proteins by using Discovery Studio 3.1 (Accelrys Inc., San Diego, CA, USA). GoldScore was selected as the scoring function, and other parameters were set as default. The image was created using PyMOL [40].

Acknowledgement This work was supported by the Project of Science and Technology Assistance in Developing Countries (KY201501006) and the Natural Science Foundation of Tianjin (17JCQNJC13500) and the Fundamental Research Funds for the Central Universities，Nankai University (63191149).

References

[1] A. Matta, R. Ralhan, Overview of current and future biologically based targeted therapies in head and neck squamous cell carcinoma, Head & neck oncology, 1 (2009) 6.

[2] M. Krug, A. Hilgeroth, Recent advances in the development of multi-kinase inhibitors, Mini reviews in medicinal chemistry, 8 (2008) 1312-1327.

[3] S. Faivre, S. Djelloul, E. Raymond, New paradigms in anticancer therapy: targeting multiple signaling pathways with kinase inhibitors, Seminars in oncology, 33 (2006) 407-420.

[4] A. Deshpande, P. Sicinski, P.W. Hinds, Cyclins and cdks in development and cancer: a perspective, Oncogene, 24 (2005) 2909-2915.

[5] M. Malumbres, M. Barbacid, Cell cycle, CDKs and cancer: a changing paradigm, Nature reviews. Cancer, 9 (2009) 153-166.

[6] F. Canduri, P.C. Perez, R.A. Caceres, W.F. de Azevedo, Jr., CDK9 a potential target for drug development, Medicinal chemistry, 4 (2008) 210-218.

[7] G.I. Shapiro, Cyclin-dependent kinase pathways as targets for cancer treatment, J Clin Oncol, 24 (2006) 1770-1783.

[8] K.C. Goh, V. Novotny-Diermayr, S. Hart, L.C. Ong, Y.K. Loh, A. Cheong, Y.C. Tan, C. Hu, R.

Jayaraman, A.D. William, E.T. Sun, B.W. Dymock, K.H. Ong, K. Ethirajulu, F. Burrows, J.M. Wood, TG02, a novel oral multi-kinase inhibitor of CDKs, JAK2 and FLT3 with potent anti-leukemic properties, Leukemia, 26 (2012) 236-243.

[9] P.L. Toogood, P.J. Harvey, J.T. Repine, D.J. Sheehan, S.N. VanderWel, H. Zhou, P.R. Keller, D.J. McNamara, D. Sherry, T. Zhu, J. Brodfuehrer, C. Choi, M.R. Barvian, D.W. Fry, Discovery of a potent and selective inhibitor of cyclin-dependent kinase 4/6, Journal of medicinal chemistry, 48 (2005) 2388-2406.

[10] J. Rader, M.R. Russell, L.S. Hart, M.S. Nakazawa, L.T. Belcastro, D. Martinez, Y.M. Li, E.L. Carpenter, E.F. Attiyeh, S.J. Diskin, S. Kim, S. Parasuraman, G. Caponigro, R.W. Schnepp, A.C. Wood, B. Pawel, K.A. Cole, J.M. Maris, Dual CDK4/CDK6 Inhibition Induces Cell-Cycle Arrest and Senescence in Neuroblastoma, Clin Cancer Res, 19 (2013) 6173-6182.

[11] J.E. Logan, N. Mostofizadeh, A.J. Desai, E. Von Euw, D. Conklin, V. Konkankit, H. Hamidi, M. Eckardt, L. Anderson, H.W. Chen, C. Ginther, E. Taschereau, P.H. Bui, J.G. Christensen, A.S. Belldegrun, D.J. Slamon, F.F. Kabbinavar, PD-0332991, a Potent and Selective Inhibitor of Cyclin-dependent Kinase 4/6, Demonstrates Inhibition of Proliferation in Renal Cell Carcinoma at Nanomolar Concentrations and Molecular Markers Predict for Sensitivity, Anticancer Res, 33 (2013) 2997-3004.

[12] R.S. Finn, J. Dering, D. Conklin, O. Kalous, D.J. Cohen, A.J. Desai, C. Ginther, M. Atefi, I. Chen, C. Fowst, G. Los, D.J. Slamon, PD 0332991, a selective cyclin D kinase 4/6 inhibitor, preferentially inhibits proliferation of luminal estrogen receptor-positive human breast cancer cell lines in vitro, Breast Cancer Research, 11 (2009).

[13] L.B. Baughn, M. Di Liberto, K. Wu, P. Toogood, T. Louie, R. Gottschalk, R. Niesvizky, H.J. Cho, S. Ely, M.A.S. Moore, S. Chen-Kiang, A novel orally active small molecule potently induces G1 arrest in primary myeloma cells and prevents tumor growth by specific inhibition of Cdk4/6., Blood, 108 (2006) 113a-114a.

[14] G.N. Hortobagyi, S.M. Stemmer, H.A. Burris, Y.S. Yap, G.S. Sonke, S. Paluch-Shimon, M. Campone, K.L. Blackwell, F. Andre, E.P. Winer, W. Janni, S. Verma, P. Conte, C.L. Arteaga, D.A. Cameron, K. Petrakova, L.L. Hart, C. Villanueva, A. Chan, E. Jakobsen, A. Nusch, O. Burdaeva, E.M. Grischke, E. Alba, E. Wist, N. Marschner, A.M. Favret, D. Yardley, T. Bachelot, L.M. Tseng, S. Blau, F. Xuan, F. Souami, M. Miller, C. Germa, S. Hirawat, J. O'Shaughnessy, Ribociclib as First-Line Therapy for HR-Positive, Advanced Breast Cancer, New Engl J Med, 375 (2016) 1738-1748.

[15] P.N. Munster, E.P. Hamilton, L.G. Estevez, R.H. De Boer, I.A. Mayer, M. Campone, S. Asano, S. Bhansali, V. Zhang, B. Hewes, D. Juric, Ph IB study of LEE011 and BYL719 in combination with letrozole in ER+, Her2-breast cancer., J Clin Oncol, 32 (2014).

[16] P. Carmeliet, Angiogenesis in life, disease and medicine, Nature, 438 (2005) 932-936.

[17] K.J. Gotink, H.M.W. Verheul, Anti-angiogenic tyrosine kinase inhibitors: what is their mechanism of action?, Angiogenesis, 13 (2010) 1-14.

[18] S. Tugues, S. Koch, L. Gualandi, X.J. Li, L. Claesson-Welsh, Vascular endothelial growth factors and receptors: Anti-angiogenic therapy in the treatment of cancer, Mol Aspects Med, 32 (2011) 88-111.

[19] N. Ferrara, H.P. Gerber, J. LeCouter, The biology of VEGF and its receptors, Nat Med, 9 (2003) 669-676.

[20] J.C. He, W. Yao, J.M. Wang, P. Schemmer, Y. Yang, Y. Liu, Y.W. Qian, W.P. Qi, J. Zhang, Q. Shen, T. Yang, TACC3 overexpression in cholangiocarcinoma correlates with poor prognosis and is a potential anti-cancer molecular drug target for HDAC inhibitors, Oncotarget, 7 (2016) 75441-75456.

[21] Z.F. Zhong, W. Tan, S.P. Wang, W.A. Qiang, Y.T. Wang, Anti-proliferative activity and cell cycle arrest induced by evodiamine on paclitaxel-sensitive and -resistant human ovarian cancer cells, Sci Rep-Uk, 5 (2015).

[22] CHAN, Edward, Michael (c/o Eli Lilly and Company, P.O. Box 6288, Indianapolis, IN 46206-6288, US) Combination therapy for cancer, WO2015130540A1, 2015, 1-56.

[23] G.C. Fletcher, R.D. Brokx, T.A. Denny, T.A. Hembrough, S.M. Plum, W.E. Fogler, C.F. Sidor, M.R. Bray, ENMD-2076 is an orally active kinase inhibitor with antiangiogenic and antiproliferative mechanisms of action, Molecular cancer therapeutics, 10 (2011) 126-137.

[24] K. Kolinsky, C. Tovar, Y.E. Zhang, A. Railkar, H. Yang, D. Carvajal, T. Nevins, W. Geng, M. Linn, K. Packman, J.J. Liu, Z. Zhang, P. Wovkulich, G. Ju, B. Higgins, Preclinical evaluation of the novel multi-targeted agent R1530, Cancer chemotherapy and pharmacology, 68 (2011) 1585-1594.

[25] A. Jindal, A. Thadi, K. Shailubhai, Hepatocellular Carcinoma: Etiology and Current and Future Drugs, Journal of clinical and experimental hepatology, 9 (2019) 221-232.

[26] J. Bollard, V. Miguela, M. Ruiz de Galarreta, A. Venkatesh, C.B. Bian, M.P. Roberto, V. Tovar, D. Sia, P. Molina-Sanchez, C.B. Nguyen, S. Nakagawa, J.M. Llovet, Y. Hoshida, A. Lujambio, Palbociclib (PD-0332991), a selective CDK4/6 inhibitor, restricts tumour growth in preclinical models of hepatocellular carcinoma, Gut, 66 (2017) 1286-1296.

[27] W.K. You, B. Sennino, C.W. Williamson, B. Falcon, H. Hashizume, L.C. Yao, D.T. Aftab, D.M. McDonald, VEGF and c-Met Blockade Amplify Angiogenesis Inhibition in Pancreatic Islet Cancer, Cancer Res, 71 (2011) 4758-4768.

[28] R. Kurzrock, S.I. Sherman, D.W. Ball, A.A. Forastiere, R.B. Cohen, R. Mehra, D.G. Pfister, E.E.W. Cohen, L. Janisch, F. Nauling, D.S. Hong, C.S. Ng, L. Ye, R.F. Gagel, J. Frye, T. Muller, M.J. Ratain, R.

Salgia, Activity of XL184 (Cabozantinib), an Oral Tyrosine Kinase Inhibitor, in Patients With Medullary Thyroid Cancer, J Clin Oncol, 29 (2011) 2660-2666.

[29] Y.T. Li, Q.X. Guo, C. Zhang, Z. Huang, T.Q. Wang, X. Wang, X. Wang, G.W. Xu, Y.H. Liu, S.Y. Yang, Y. Fan, R. Xiang, Discovery of a highly potent, selective and novel CDK9 inhibitor as an anticancer drug candidate, Bioorg Med Chem Lett, 27 (2017) 3231-3237.

[30] Z.S. Zhan, J. Ai, Q.F. Liu, Y.C. Ji, T.T. Chen, Y.C. Xu, M.Y. Geng, W.H. Duan, Discovery of Anilinopyrimidines as Dual Inhibitors of c-Met and VEGFR-2: Synthesis, SAR, and Cellular Activity, Acs Med Chem Lett, 5 (2014) 673-678.

[31] M. McConville, D.F. Bradley, K. Zhou, D.J. Schiffrin, I.A. O'Neil, Selective trioxolane based bifunctional molecular linkers for covalent heme surface functionalisation, Chem Commun, 50 (2014) 186-188.

[32] J.Y. Le Brazidec, A. Pasis, B. Tam, C. Boykin, D.P. Wang, D.J. Marcotte, G. Claassen, J.H. Chong, J.H. Chao, J.H. Fan, K. Nguyen, L. Silvian, L. Ling, L. Zhang, M. Choi, M. Teng, N. Pathan, S. Zhao, T. Li, A. Taveras, Structure-based design of 2,6,7-trisubstituted-7H-pyrrolo[2,3-d]pyrimidines as Aurora kinases inhibitors, Bioorg Med Chem Lett, 22 (2012) 4033-4037.

[33] Y.T. Li, X.H. Luo, Q.X. Guo, Y.W. Nie, T.Q. Wang, C. Zhang, Z. Huang, X. Wang, Y.H. Liu, Y.A. Chen, J.Y. Zheng, S.Y. Yang, Y. Fan, R. Xiang, Discovery of &ITN&IT1-(4-((7-Cyclopentyl-6-(dimethylcarbamoyl)-7&ITH&IT-pyrrolo[2,3-&ITd&IT]pyrimidin-2-yl)amino)phenyl)-&ITN&IT8-hydroxyoctanediamide as a Novel Inhibitor Targeting Cyclin-dependent Kinase 4/9 (CDK4/9) and Histone Deacetlyase 1 (HDAC1) against Malignant Cancer, Journal of medicinal chemistry, 61 (2018) 3166-3192.

[34] T.K. Mohamed, R.Z. Batran, S.A. Elseginy, M.M. Ali, A.E. Mahmoud, Synthesis, anticancer effect and molecular modeling of new thiazolylpyrazolyl coumarin derivatives targeting VEGFR-2 kinase and inducing cell cycle arrest and apoptosis, Bioorganic chemistry, 85 (2019) 253-273.

[35] A.E.S. Mghwary, E.M. Gedawy, A.M. Kamal, S.M. Abuel-Maaty, Novel thienopyrimidine derivatives as dual EGFR and VEGFR-2 inhibitors: design, synthesis, anticancer activity and effect on cell cycle profile, J Enzym Inhib Med Ch, 34 (2019) 838-852.

[36] Y.S. Duan, S. Zhang, L.L. Wang, X. Zhou, Q.H. He, S. Liu, K. Yue, X.D. Wang, Targeted silencing of CXCR4 inhibits epithelial-mesenchymal transition in oral squamous cell carcinoma, Oncol Lett, 12 (2016) 2055-2061.

[37] S. Yang, L. Zhao, J.H. Yang, D.G. Chai, M. Zhang, J. Zhang, X.H. Ji, T.H. Zhu, delta EF1 represses BMP-2-induced differentiation of C2C12 myoblasts into the osteoblast lineage, J Biomed Sci, 14 (2007) 663-679.

[38] Z. Huang, W. Zhou, Y. Li, M. Cao, T. Wang, Y. Ma, Q. Guo, X. Wang, C. Zhang, C. Zhang, W. Shen, Y. Liu, Y. Chen, J. Zheng, S. Yang, Y. Fan, R. Xiang, Novel hybrid molecule overcomes the limited response of solid tumours to HDAC inhibitors via suppressing JAK1-STAT3-BCL2 signalling, Theranostics, 8 (2018) 4995-5011.

[39] N. Eswar, D. Eramian, B. Webb, M.Y. Shen, A. Sali, Protein structure modeling with MODELLER, Methods in molecular biology, 426 (2008) 145-159.

[40] W.L. Delano, The pymol molecular graphics system, schrödinger, llc: New york, 2014.

Table 1. Structure and inhibitory activity of **5A-K,6D,6F,6H,6J,6K,14A-K** against CDK4 and VEGFR2 at 1 μM[a]

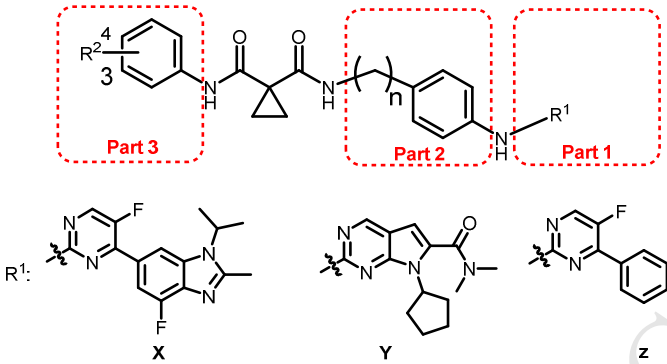

Compounds	R^1	n	R^2	Inhibition% at 1 μM	
				CDK4	VEGFR2
Abemaciclib	-			99	-
Cabozantinib	-			-	101
Roxyl-ZV-5A	X	0	3-F	96	90
Roxyl-ZV-5B	X	0	4-F	98	91
Roxyl-ZV-5C	X	0	3-Cl	74	90
Roxyl-ZV-5D	X	0	4-Cl	76	74
Roxyl-ZV-5E	X	0	3- Br	83	90
Roxyl-ZV-5F	X	0	4-Br	90	91
Roxyl-ZV-5G	X	0	3-CF_3	31	80

Roxyl-ZV-5H	X	0	4-CF_3	74	80
Roxyl-ZV-5I	X	0	3-CH_3	97	95
Roxyl-ZV-5J	X	0	4-CH_3	97	95
Roxyl-ZV-5K	X	0	3-CF_3, 4-Cl	34	68
Roxyl-ZV-6D	X	1	4-Cl	88	91
Roxyl-ZV-6F	X	1	4-Br	93	90
Roxyl-ZV-6H	X	1	4-CF_3	37	74
Roxyl-ZV-6J	X	1	4-CH_3	97	95
Roxyl-ZV-6K	X	1	3-CF_3, 4-Cl	51	57
4d	Y	0	4-F	102	0
4f	Y	0	4-Cl	65	5
4h	Y	0	4-Br	48	26
4j	Y	0	4-CH_3	62	9
4l	Y	0	4-CF_3	32	1
Roxyl-ZV-14A	Z	0	3-F	79	69
Roxyl-ZV-14B	Z	0	4-F	69	84
Roxyl-ZV-14C	Z	0	3-Cl	50	60
Roxyl-ZV-14D	Z	0	4-Cl	21	59

Roxyl-ZV-14E	Z	0	3- Br	34	55
Roxyl-ZV-14F	Z	0	4-Br	24	52
Roxyl-ZV-14G	Z	0	3-CF_3	13	46
Roxyl-ZV-14H	Z	0	4-CF_3	31	56
Roxyl-ZV-14I	Z	0	3-CH_3	75	73
Roxyl-ZV-14J	Z	0	4-CH_3	81	78
Roxyl-ZV14K	Z	0	3-CF_3, 4-Cl	8	41

[a] Inhibition values were determined using KinaseProfiler by Eurofins. The data represent the mean values of two independent experiments. [b] indicated that data were from our previous work in reference 24

Table 2. *In vitro* growth inhibitory activities of compound **Roxyl-ZV-5J** against human cancer cell lines.[a]

Cell lines	IC_{50} (nM)		
	Roxyl-ZV-5J	**Cabozantinib**	**Abemaciclib**
SiHa	50	7940	861
HeLa	72	>10000	768
MDA-MB-231	38	5080	62
T-47D	16	4790	145
HUVEC	36	7670	403

[a] The IC_{50} values were shown in the forms. The cytotoxic effects were assayed using CCK-8 assay.

Table 3. Analysis of the Main Pharmacokinetic Parameters for **Roxyl-ZV-5J** after an Oral and an Intravenous Administration (n = 5 for each group)[a]

Parameters	iv	p.o
AUC(0-t)(mg/L*h)	10	6
AUC(0-∞)	11	6
AUMC(0-t)	17	21
MRT(0-t)(h)	2	4
VRT(0-t)(h^2)	2	7
$t_{1/2}$(h)	2	3
Tmax(min)	5	120
V(L/kg)	2	6
CL(L/h/kg)	1	2
Cmax(mg/L)	7	1
F(%)[a]		60

[a] F (oral bioavailability) = $AUC_{0-t(po)}$ ×/$AUC_{0-t(iv)}$ × 100%

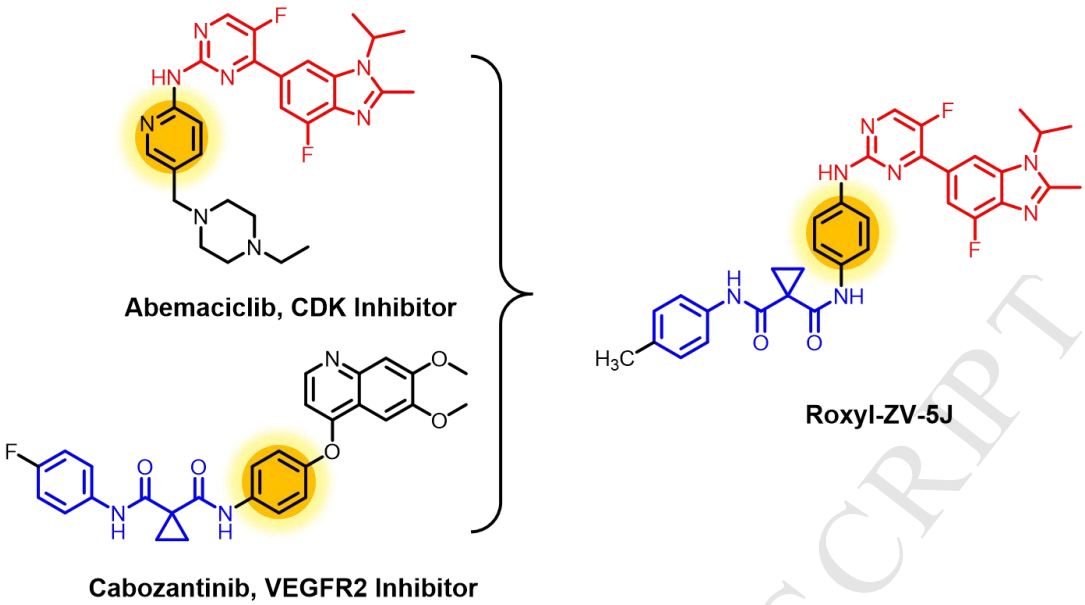

Figure 1. Schematic showing design for a novel hybrid inhibitor.

Scheme 1. Synthesis of Compounds **5A-K,6D,6F,6H,6J,6K**.

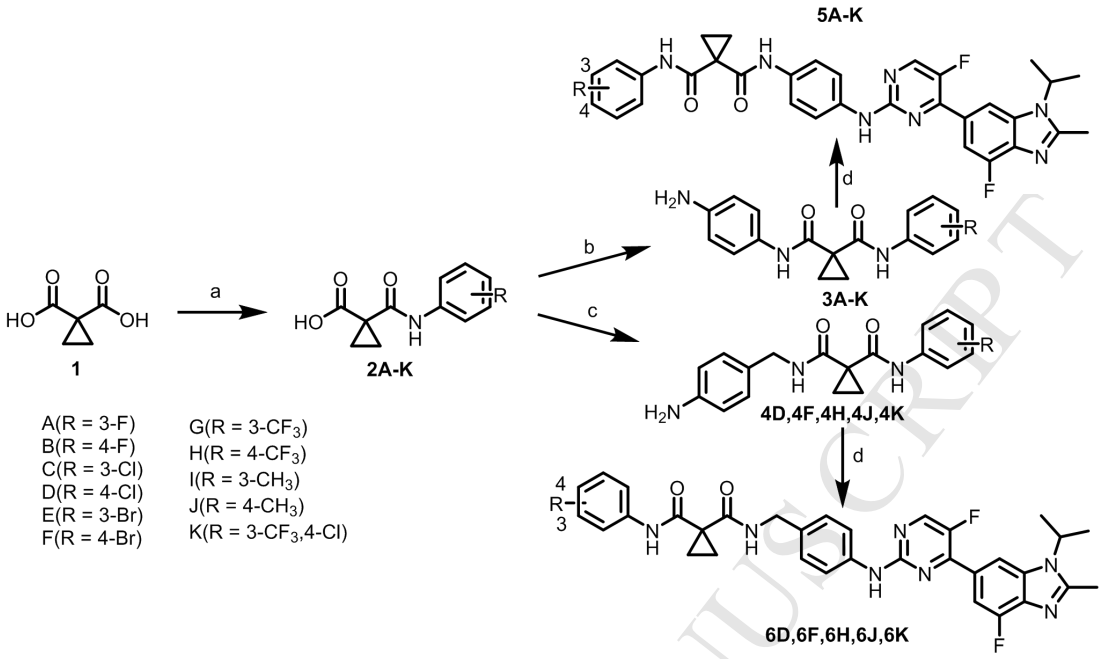

Reagents and conditions: (a) $SOCl_2$, Et_3N, THF, then aniline or substituted aniline, 55-84% yield; (b) *p*-phenylenediamine, EDCI, HOBt, DIEA, rt, 18-85% yield; (c) 4-(aminomethyl)aniline dihydrochloride, EDCI, HOBt, DIEA, rt, 50-86% yield; (d) 6-(2-chloro-5-fluoropyrimidin-4-yl)-4-fluoro-1-isopropyl-2-methyl-1H-benzo[d]imidazole(**7**), $Pd(AcO)_2$, BINAP, Cs_2CO_3, 100 °C, 40-70% yield.

Scheme 2. Synthesis of intermediate compound **13**[a].

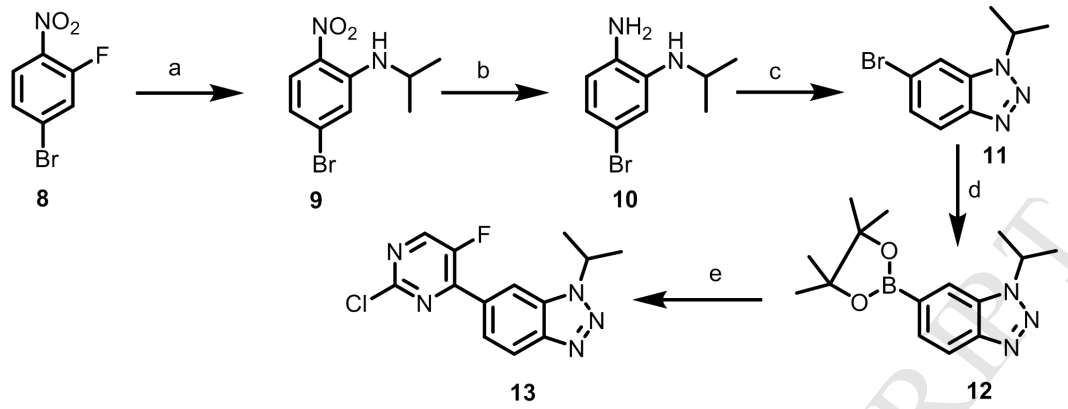

[a]Reagents and conditions: (a) isopropylamine, K_2CO_3, DMF, RT, 96% yield; (b)CH_3COOH, Fe, 70 °C, 91% yield; (c) conc.HCl, $NaNO_2$, 0 °C, 78% yield; (d) bis(pinacolato)diboron, $PdCl_2$(pddf), KOAc, 95 °C, 67% yield; (e) 2,4-dichloro-5-fluoropyrimidine, $PdCl_2$(pddf), $NaHCO_3$, 100 °C, 59% yield.

Scheme 3. Synthesis of Compounds **14A-K** [a].

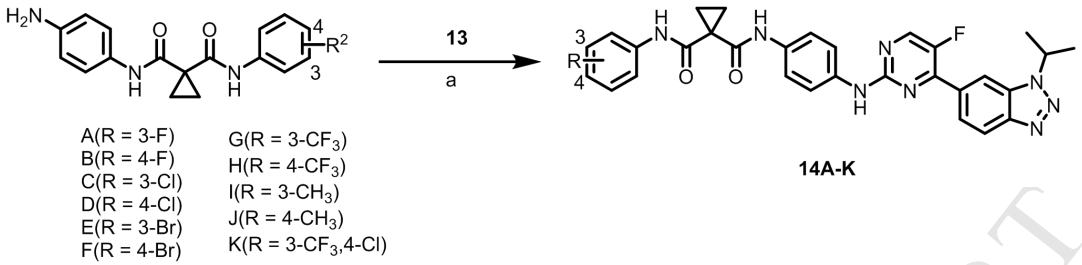

A(R = 3-F)
B(R = 4-F)
C(R = 3-Cl)
D(R = 4-Cl)
E(R = 3-Br)
F(R = 4-Br)

G(R = 3-CF_3)
H(R = 4-CF_3)
I(R = 3-CH_3)
J(R = 4-CH_3)
K(R = 3-CF_3,4-Cl)

[a]Reagents and conditions: (a) $Pd(AcO)_2$, BINAP, Cs_2CO_3, 100 °C, 40-65%.

Table 1. Structure and inhibitory activity of **5A-K,6D,6F,6H,6J,6K,14A-K** against CDK4 and VEGFR2 at 1 μM[a]

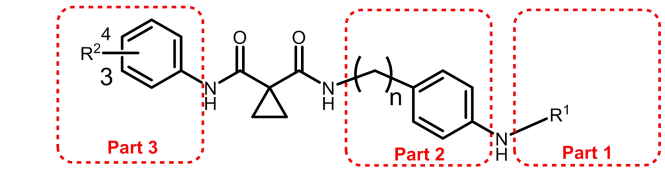

R^1:

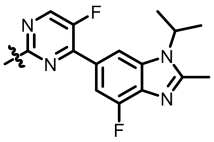

X

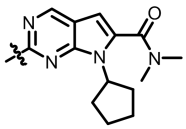

Y

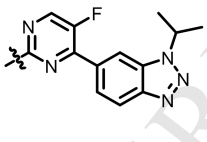

z

Compounds	R^1	n	R^2	Inhibition% at 1 μM	
				CDK4	VEGFR2
Abemaciclib	-			99	-
Cabozantinib	-			-	101
Roxyl-ZV-5A	X	0	3-F	96	90
Roxyl-ZV-5B	X	0	4-F	98	91
Roxyl-ZV-5C	X	0	3-Cl	74	90
Roxyl-ZV-5D	X	0	4-Cl	76	74
Roxyl-ZV-5E	X	0	3- Br	83	90
Roxyl-ZV-5F	X	0	4-Br	90	91
Roxyl-ZV-5G	X	0	3-CF_3	31	80
Roxyl-ZV-5H	X	0	4-CF_3	74	80
Roxyl-ZV-5I	X	0	3-CH_3	97	95
Roxyl-ZV-5J	X	0	4-CH_3	97	95
Roxyl-ZV-5K	X	0	3-CF_3, 4-Cl	34	68

Roxyl-ZV-6D	X	1	4-Cl	88	91
Roxyl-ZV-6F	X	1	4-Br	93	90
Roxyl-ZV-6H	X	1	4-CF_3	37	74
Roxyl-ZV-6J	X	1	4-CH_3	97	95
Roxyl-ZV-6K	X	1	3-CF_3, 4-Cl	51	57
4d	Y	0	4-F	102	0
4f	Y	0	4-Cl	65	5
4h	Y	0	4-Br	48	26
4j	Y	0	4-CH_3	62	9
4l	Y	0	4-CF_3	32	1
Roxyl-ZV-14A	Z	0	3-F	79	69
Roxyl-ZV-14B	Z	0	4-F	69	84
Roxyl-ZV-14C	Z	0	3-Cl	50	60
Roxyl-ZV-14D	Z	0	4-Cl	21	59
Roxyl-ZV-14E	Z	0	3- Br	34	55
Roxyl-ZV-14F	Z	0	4-Br	24	52
Roxyl-ZV-14G	Z	0	3-CF_3	13	46
Roxyl-ZV-14H	Z	0	4-CF_3	31	56
Roxyl-ZV-14I	Z	0	3-CH_3	75	73
Roxyl-ZV-14J	Z	0	4-CH_3	81	78
Roxyl-ZV14K	Z	0	3-CF_3, 4-Cl	8	41

[a] Inhibition values were determined using KinaseProfiler by Eurofins. The data represent the mean values of two independent experiments. [b] indicated that data were from our previous work in reference 24

Table 2. *In vitro* growth inhibitory activities of compound **Roxyl-ZV-5J** against human cancer cell lines.[a]

Cell lines	IC_{50} (nM)		
	Roxyl-ZV-5J	**Cabozantinib**	**Abemaciclib**
SiHa	50	7940	861
HeLa	72	>10000	768
MDA-MB-231	38	5080	62
T-47D	16	4790	145
HUVEC	36	7670	403

[a] The IC_{50} values were shown in the forms. The cytotoxic effects were assayed using CCK-8 assay.

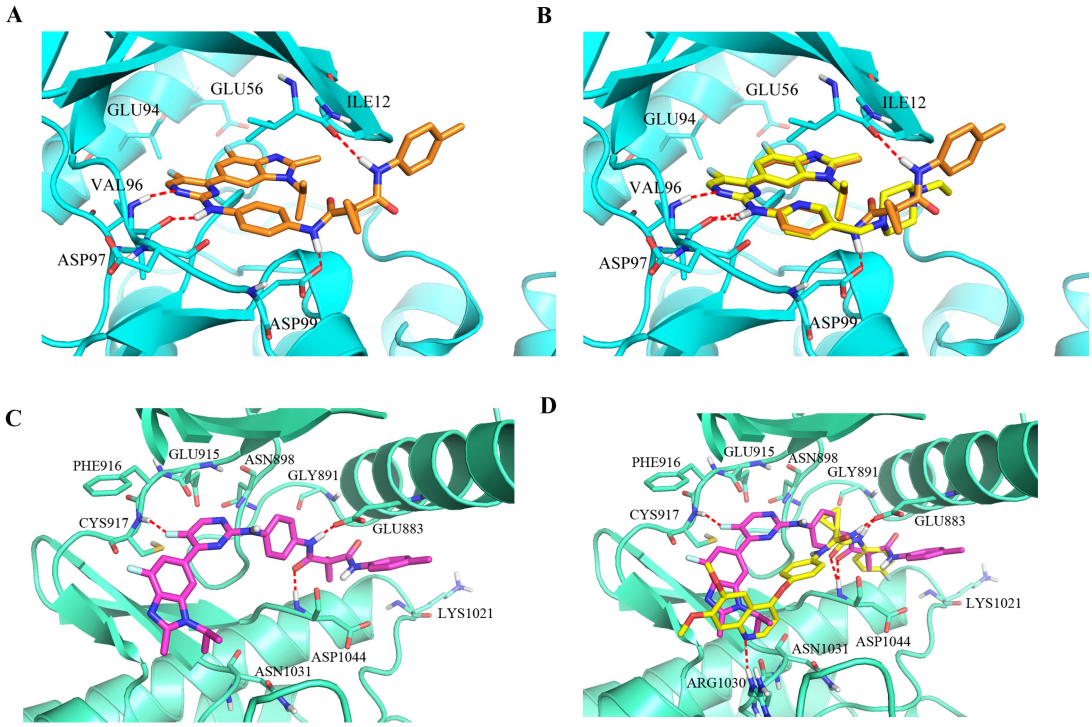

Figure 2. Representation of the predicted binding modes of compounds with CDK4 and VEGFR2 kinase domain. (A) and (B) Representation of the predicted binding modes of **Roxyl-ZV-5J** (orange) and Abemaciclib (yellow) in the ATP pocket of CDK4 which employed CDK6 (PDB entry 4EZ5) as the template for homology modeling. (C) and (D) Predicted binding mode of compound **Roxyl-ZV-5J** (purple) and cabozantinib (yellow) with VEGFR2. The crystal structure of VEGFR2 was taken from the RCSB Protein Data Bank (PDB entry: 2OH4). Dash lines indicated the H-bond interaction between compounds and enzymes.

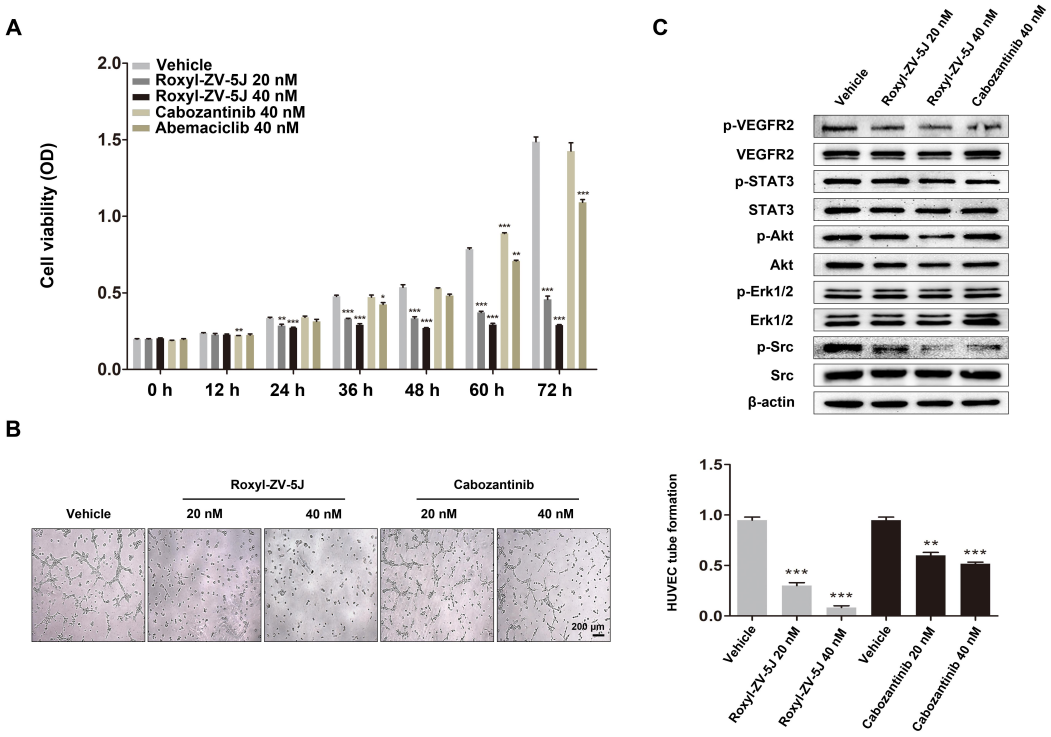

Figure 3. Roxyl-ZV-5J attenuated the proliferation and tube formation of HUVEC via VEGFR2-dependent signaling pathways. (A) **Roxyl-ZV-5J** attenuated the proliferation of HUVEC cells in dose- and time-dependent manner compared to cabozantinib, abemaciclib or vehicle group by cell viability assay. (B) **Roxyl-ZV-5J** inhibited tube formation of HUVEC compared to cabozantinib by tube formation assay. (C) **Roxyl-ZV-5J** significantly restrained the expression level of p-VEGFR2, p-STAT3, p-Akt and p-Erk1/2 compared to cabozantinib by western blot assay. HUVEC cells were treated with different concentrations of **Roxyl-ZV-5J** and Cabozantinib for 48 h. Anti-β-actin was used as a loading control.

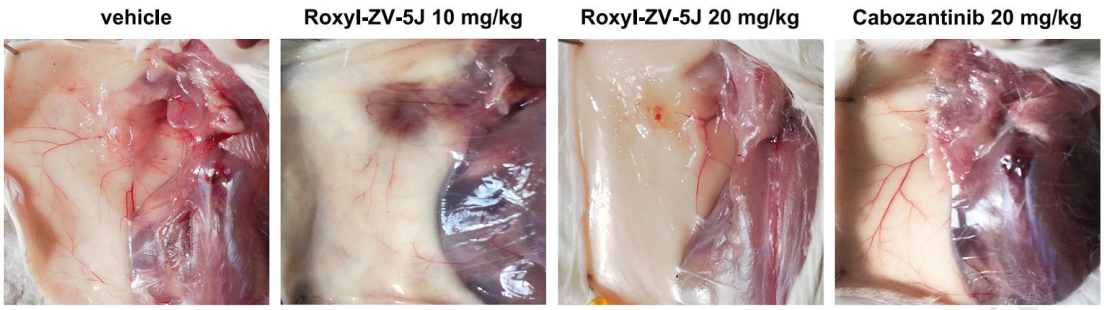

Figure 4. Roxyl-ZV-5J inhibited the angiogenesis *in vivo*. Roxyl-ZV-5J inhibited the formation of new blood vessels in Balb/c mice by Matrigel plug assay.

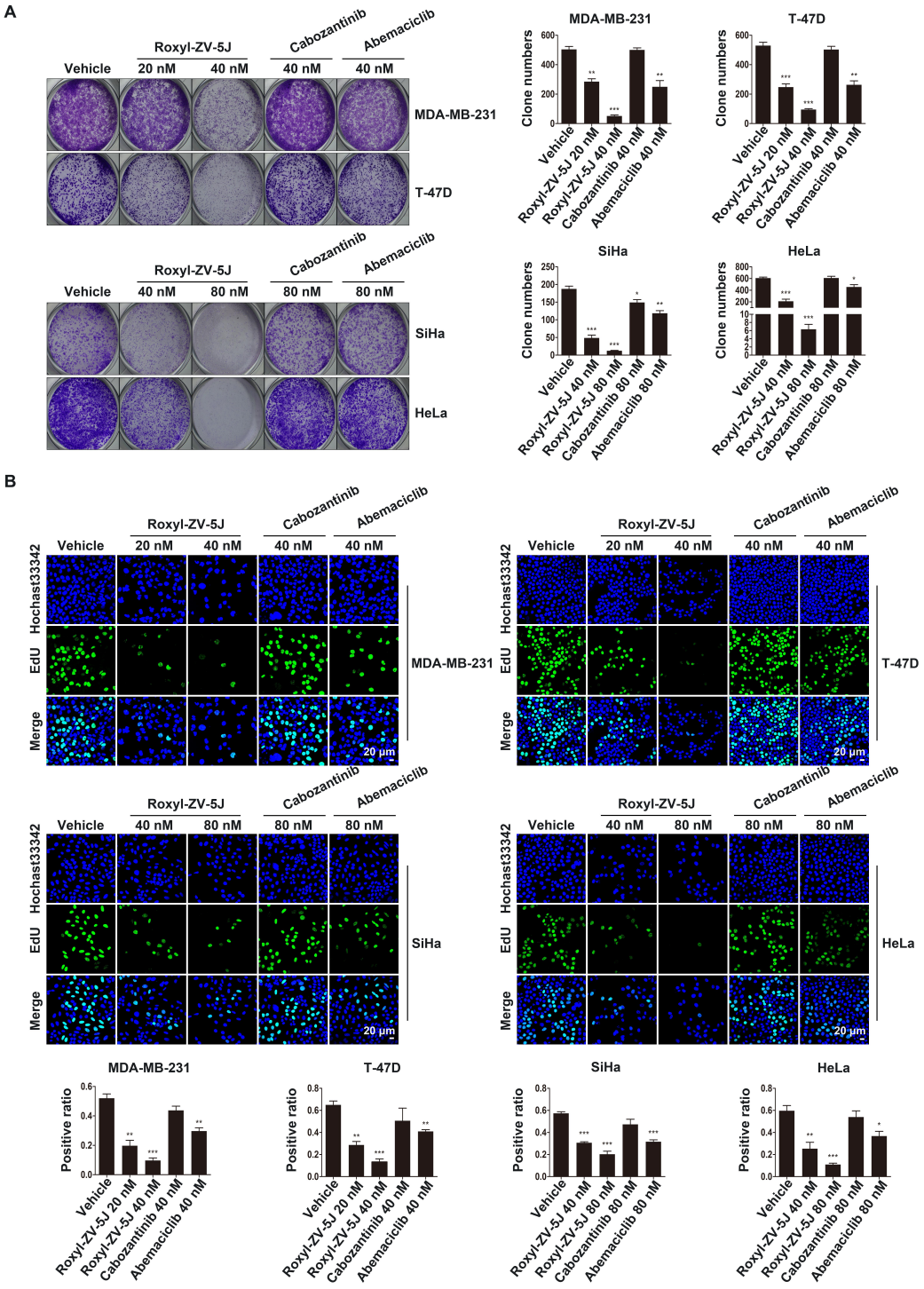

Figure 5. Roxyl-ZV-5J inhibited the proliferation against breast cancer and ovarian cancer *in vitro*. (A) **Roxyl-ZV-5J** effectively inhibited the proliferation of MDA-MB-231, T47D, SiHa and HeLa cells compared to cabozantinib, Abemaciclib and vehicle group by colony formation assay. (B) **Roxyl-ZV-5J** significantly

restrained the proliferation of cancer cells compared to other groups by EdU proliferation assay. MDA-MB-231, T47D, SiHa and HeLa cells were treated with different concentrations of **Roxyl-ZV-5J**, cabozantinib, abemaciclib or vehicle respectively for 48 h. Green signals were stained by Alexa-488 and cell nuclei was stained by Hoechst 33342.

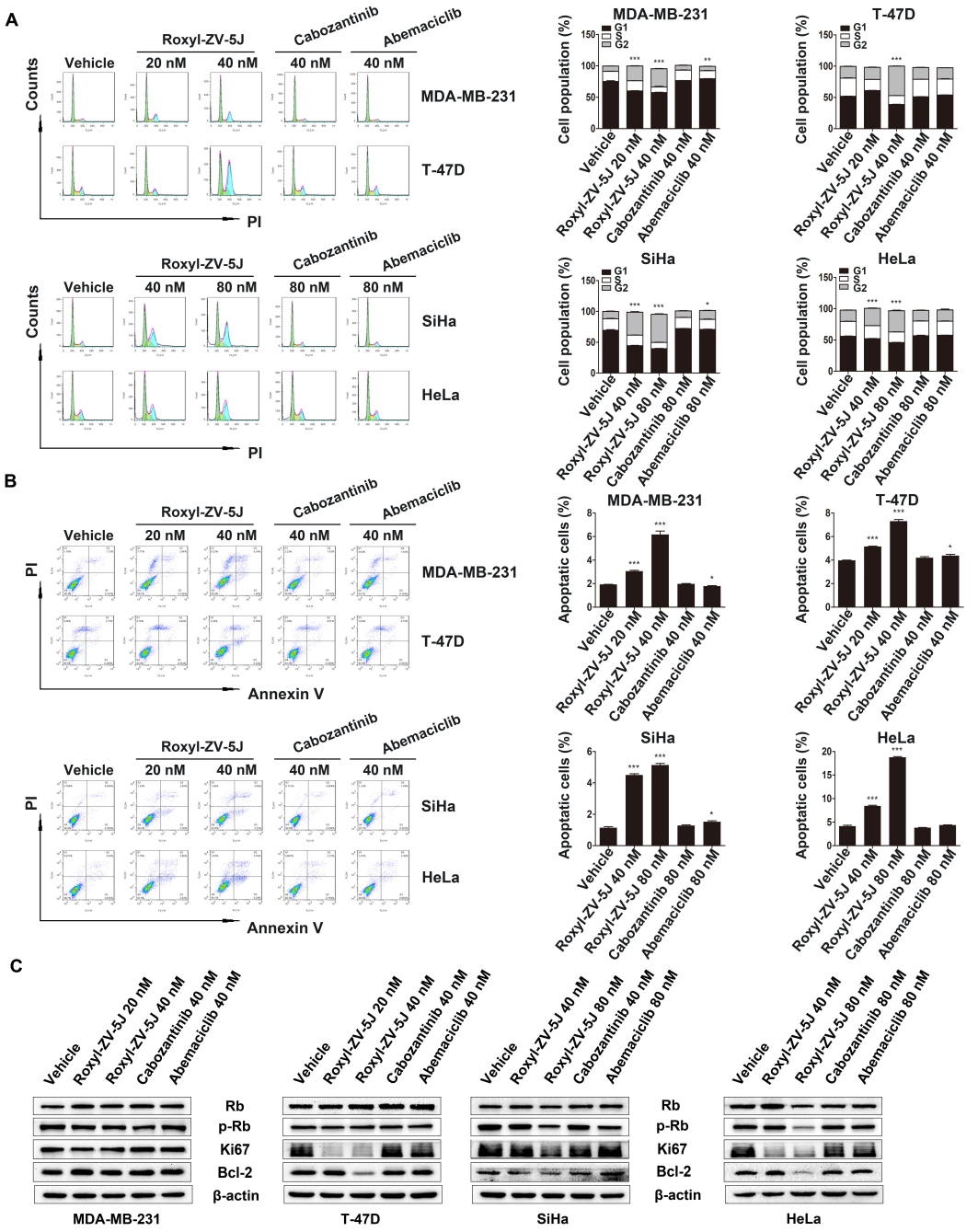

Figure 6. Roxyl-ZV-5J induced cell cycle arrest and apoptosis against breast cancer and ovarian cancer *in vitro*. (A) **Roxyl-ZV-5J** induced G_2 arrest remarkably accompanied by reduction of G_0/G_1 and S phase in MDA-MB-231, T47D, SiHa and HeLa cells by flow cytometry assay. (B) **Roxyl-ZV-5J** increased the apoptosis proportion compared to cabozantinib, abemaciclib or vehicle group in MDA-MB-231, T47D, SiHa and HeLa cells by flow cytometry assay. (C) **Roxyl-ZV-5J** decreased the expression level of p-Rb, Ki67 and Bcl-2 by western blot assay. MDA-MB-231, T47D, SiHa and HeLa cells were treated with different

concentrations of **Roxyl-ZV-5J,** cabozantinib, abemaciclib or vehicle for 48 h. Anti-β-actin was used as a loading control.

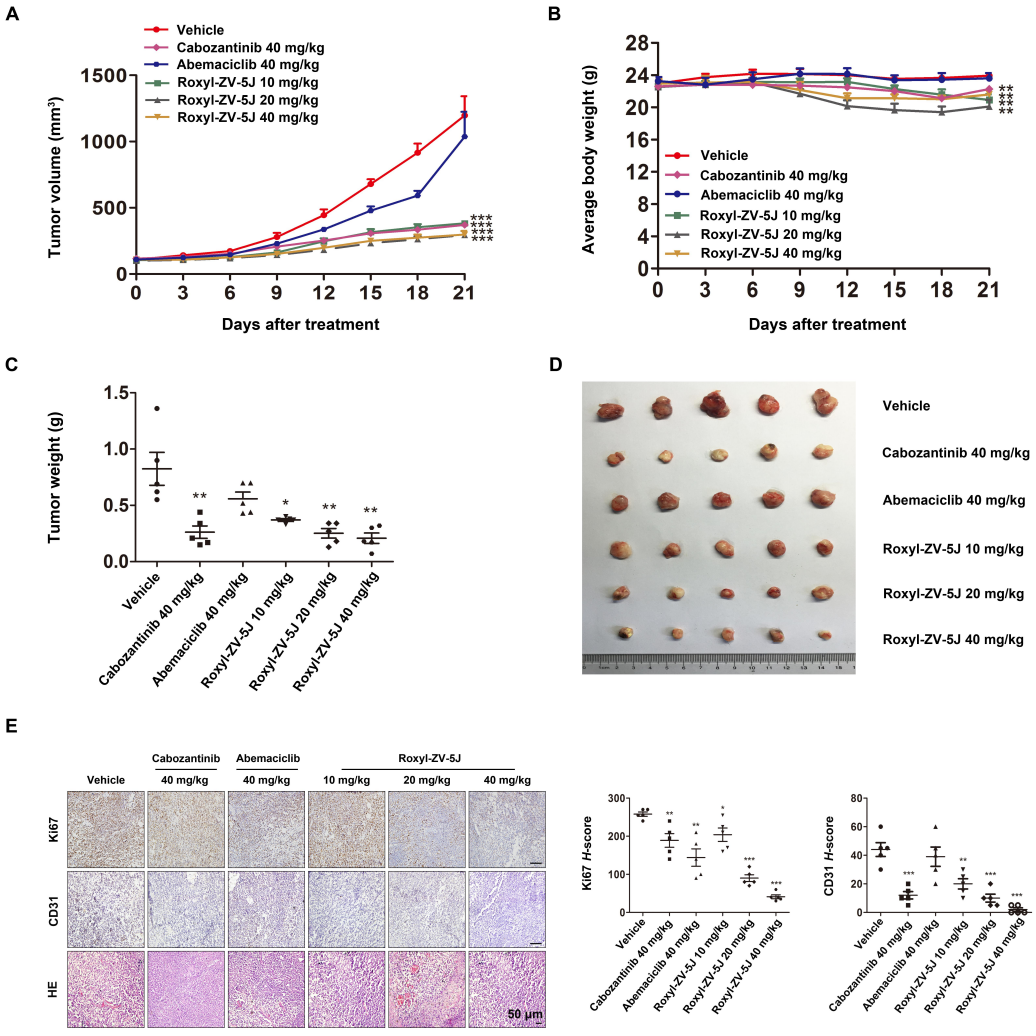

Figure 7. Roxyl-ZV-5J significantly inhibits the growth and angiogenesis of cervical cancer in SiHa tumor xenograft models. (A) The growth curve of **Roxyl-ZV-5J** (10 mg/kg, 20 mg/kg, 40 mg/kg), cabozantinib 40 mg/kg, abemaciclib 40 mg/kg or vehicle treated xenograft tumor orally once per day. Tumor growth in **Roxyl-ZV-5J** groups was significantly inhibited compared to other groups at day 21. (B) The average body weight of xenograft tumor mice after treated with different concentrations of **Roxyl-ZV-5J**, cabozantinib, abemaciclib or vehicle. (C) The average tumor weight of excised tumors at day 21. Tumors in **Roxyl-ZV-5J** groups were obviously lighter compared to other groups. (D) Photograph of excised tumors with respective mice at day 21. Treatment with **Roxyl-ZV-5J** resulted in a decrease in tumor volume when compared to other groups (cabozantinib 40mg/kg, abemaciclib 40mg/kg or vehicle). (E) IHC staining showed that the expression level of Ki67 and

CD31 was decreased in **Roxyl-ZV-5J** groups in a dose-dependent relation, compared to other groups.

Table 3. Analysis of the Main Pharmacokinetic Parameters for **Roxyl-ZV-5J** after an Oral and an Intravenous Administration (n = 5 for each group)[a]

Parameters	iv	p.o
AUC(0-t)(mg/L*h)	10	6
AUC(0-∞)	11	6
AUMC(0-t)	17	21
MRT(0-t)(h)	2	4
VRT(0-t)(h^2)	2	7
$t_{1/2}$(h)	2	3
Tmax(min)	5	120
V(L/kg)	2	6
CL(L/h/kg)	1	2
Cmax(mg/L)	7	1
F(%)[a]		60

[a] F (oral bioavailability) = $AUC_{0-t(po)} \times / AUC_{0-t(iv)} \times 100\%$

- A series of novel multi-kinase inhibitors targeting CDK4 and VEGFR2 were designed, synthesized and evaluated.
- **Roxyl-ZV-5J** with potent and balanced activities against both CDK4 and VEGFR2 at the nanomolar level, exhibited improved anti-proliferative and anti-angiogenesis activities over positive drugs *in vitro* and *in vivo*.
- For the first time our results demonstrated that dual CDK-VEGFR2 pathways inhibition achieved with a single molecule could be a promising agent applicable for cancer therapy.